

~~CONFIDENTIAL~~UNCLASSIFIED
AUG 12 1953

NACA RM E52K10

The NACA logo consists of the acronym "NACA" in a bold, sans-serif font, centered within a stylized aircraft wing profile.

RESEARCH MEMORANDUM

ALTITUDE WIND TUNNEL INVESTIGATION OF THE PROTOTYPE
J40-WE-8 TURBOJET ENGINE WITHOUT AFTERBURNER

By John E. McAulay and Harold R. Kaufman

Lewis Flight Propulsion Laboratory
Cleveland, Ohio

CLASSIFICATION CHANGED

To UNCLASSIFIED

By authority of TPA - #17 ^{Effect.} Date 3/10/60
JS4

CLASSIFIED DOCUMENT

This material contains information affecting the National Defense of the United States within the meaning of the espionage laws, Title 18, U.S.C., Secs. 793 and 794, the transmission or revelation of which in any manner to an unauthorized person is prohibited by law.

NATIONAL ADVISORY COMMITTEE
FOR AERONAUTICS

WASHINGTON

August 6, 1953

NACA LIBRARY

Lewis Flight Propulsion Laboratory
Langley Field, Va.

~~CONFIDENTIAL~~

NATIONAL ADVISORY COMMITTEE FOR AERONAUTICS

RESEARCH MEMORANDUM

ALTITUDE WIND TUNNEL INVESTIGATION OF THE PROTOTYPE J40-WE-8

TURBOJET ENGINE WITHOUT AFTERBURNER

By John E. McAulay and Harold R. Kaufman

2733

SUMMARY

An investigation was conducted in the Lewis altitude wind tunnel to evaluate the performance characteristics of the prototype J40-WE-8 turbojet engine without an afterburner. Data were obtained with an electronic control operative and inoperative. The performance data were obtained at altitudes from 15,000 to 60,000 feet and flight Mach numbers of 0.17 to 1.68.

Fixed-exhaust-nozzle data showed that in general increasing altitude resulted in an increase in corrected net thrust at a given corrected engine speed. These data also showed that above a corrected engine speed of 7000 rpm a change in altitude at a given corrected engine speed had no effect on the corrected air flow. A method is presented to define the effect of changes in engine operating and flight conditions on the pumping and air-flow characteristics and the combustion efficiency. This made it possible to calculate thrust and fuel flow for conditions other than those at which the data were obtained. These calculated values were in close agreement with values obtained in the direct investigation.

INTRODUCTION

As part of a comprehensive investigation of the J40 turbojet engine conducted at the NACA Lewis altitude wind tunnel, the steady-state engine performance of the prototype J40-WE-8 turbojet engine without afterburner was obtained and is presented herein. Preliminary performance tests of an earlier model, the XJ40-WE-6, revealed a severe surge condition in the compressor at high corrected engine speeds (reference 1). A basic redesign of the compressor and other modifications in the compressor and the combustor were incorporated in the XJ40-WE-6 turbojet engine (references 2 and 3). In this report the modified engine is designated "the prototype J40-WE-8 without afterburner."

Performance data presented herein were obtained over a range of engine speeds at five fixed settings of the variable-area exhaust nozzle. These data were obtained at altitudes from 15,000 to 45,000 feet and at

flight Mach numbers of 0.62 and 0.99. Data were also obtained with an open exhaust nozzle at altitudes of 50,000 and 55,000 feet at a flight Mach number of 0.62. In addition, some data were obtained at flight Mach numbers as high as 1.68 at altitudes of 55,000 and 60,000 feet by a different method of simulation wherein engine-inlet temperature and pressure, but not tunnel static or altitude ambient pressure, are reproduced. The use of the engine pumping characteristics made it possible to calculate engine performance for a greater range of flight Mach numbers and altitudes than were experimentally investigated.

The data obtained at fixed settings of the variable-area exhaust nozzle are presented in both graphical and tabular form. In addition, data with an electronic engine control operative are also presented in tabular form.

APPARATUS AND INSTALLATION

The prototype J40-WE-8 turbojet engine without afterburner has a static sea-level thrust rating of 7500 pounds at an engine speed of 7260 rpm and a turbine-inlet temperature of 1885° R (1425° F). At this operating condition the air flow is approximately 142 pounds per second. The engine components included a divided inlet duct (fig. 1), an eleven-stage axial-flow compressor, an annular combustor, a two-stage turbine, a tail pipe, and a variable-area exhaust nozzle. Without the afterburner the engine length is 186 inches and the maximum diameter 43 inches. The dry weight of the engine and accessories is about 3000 pounds.

The engine was mounted on a wing section that spanned the 20-foot-diameter test section of the altitude wind tunnel (fig. 2). Dry refrigerated air was supplied to the engine from the tunnel make-up air system through a duct which was divided and connected to the engine inlets. Throttle valves installed in the main duct permitted regulation of the pressure at the engine inlet.

Engine thrust and drag measurements by the tunnel balance scales were made possible by the frictionless slip joint located in the main duct upstream of the engine. Instrumentation for measuring pressures and temperatures was installed at various stations in the engine (fig. 3). Pressure measurements at the exhaust-nozzle inlet were available for only a small portion of the investigation. Turbine-inlet radial temperature distributions were determined by ten traversable sonic-flow thermocouple probes.

PROCEDURE

Engine performance data presented in this report were obtained at the flight conditions shown by the following table:

Altitude (ft)	Flight Mach number						
	0.17	0.62	0.92	0.99	1.19	1.46	1.68
15 $\times 10^3$	x	x *					
35	x	x *		x *			
45	x	*					
50	x						
55	x	✓	✓		✓		✓
60		✓	✓		✓	✓	✓

x control data

* fixed exhaust-nozzle data

✓ rated speed, "military" and "normal"
turbine-inlet temperatures

The control scheduled data included open-exhaust-nozzle operating lines. The fixed-exhaust-nozzle data were obtained at projected exhaust-nozzle areas of 367, 421, 449, 479, and 535 square inches at several engine speeds for each exhaust-nozzle area. The fixed-exhaust-nozzle data are given in table I. Similarly, the control data are given in table II but are not presented graphically because standard inlet temperatures could not be maintained for several flight conditions.

In order to obtain the various flight conditions, the air flow through the make-up air duct was throttled from approximately sea-level pressure to a total pressure at the engine inlet corresponding to the desired flight Mach number at a given altitude. For most of the runs, the tunnel pressure was set at the desired altitude ambient pressure. In the calculation of flight Mach number, complete ram-pressure recovery at the engine inlet was assumed. The temperature of the inlet air approximated NACA standard values except that the minimum temperature obtained was about 440° R. The engine fuel used was MIL-F-5624 having a lower heating value of 18,700 Btu per pound and a hydrogen-carbon ratio of 0.171. The fuel temperature entering the engine fuel system was about 80° F.

The altitude at which standard altitude pressure could be maintained is limited by exhauster capacity. To extend the range of the

investigation to higher flight Mach numbers and altitudes, a technique was used wherein the engine performance could be obtained irrespective of tunnel pressure, as long as the tunnel pressure was less than the exhaust-gas total pressure. The engine-inlet pressures and temperatures which would exist at these flight conditions were reproduced while the pressure altitude in the tunnel test section was maintained at any convenient value. The variable-area exhaust nozzle was adjusted as necessary to obtain the desired values of engine temperature ratio. As indicated in reference 4, for given engine-inlet conditions and fixed engine speed, the engine air flow, fuel flow, and pressure ratio are not dependent on the ambient-air pressure for operation at a given engine-temperature ratio. The thrust was calculated from measured values of turbine-outlet pressure and temperature and engine air flow by the method given in appendix A.

RESULTS AND DISCUSSION

Generalized Performance

Typical engine performance data obtained at a flight Mach number of 0.62 and at two exhaust-nozzle areas are shown for altitudes from 15,000 to 55,000 feet in figure 4. The two exhaust-nozzle areas chosen were the largest and smallest at which a full range of engine speeds was obtained. These data have been corrected by the factors δ and θ derived in reference 5 and defined in appendix A.

The effect of altitude on corrected air flow is presented in figures 4(a) and 4(b). At corrected engine speeds above 7000 rpm, the data generalized to a single curve; however, at corrected engine speeds below 7000 rpm, the corrected air flow decreased as altitude was increased at a given corrected engine speed.

The corrected fuel flow (figs. 4(c) and 4(d)), the corrected specific fuel consumption (figs. 4(e) and 4(f)), and the corrected exhaust-gas temperature (figs. 4(g) and 4(h)) increased as altitude was increased at a given corrected engine speed.

Decreases in compressor and turbine efficiencies resulting from the lower Reynolds numbers at the higher altitudes required an increase in corrected enthalpy rise per pound across the engine to maintain the same corrected engine speed. Higher compressor pressure ratios resulted from the higher corrected temperatures at the turbine inlet (reflected by turbine-outlet temperatures). At high corrected engine speeds, the corrected air flow did not vary appreciably with compressor pressure ratio and no shift in the compressor characteristic curves occurred with altitude; hence, the corrected air flow generalized. At lower corrected

2733
engine speeds (below 7000 rpm), the effect of higher compressor pressure ratio and the shift in the compressor characteristics resulted in lower corrected air flows for higher altitudes.

Examination of the data shows that corrected enthalpy rise across the engine increased with altitude as a result of the higher corrected temperature rise across the engine even at low speeds where the corrected air flow decreased. This corrected enthalpy rise required an increase in corrected fuel flow. However, as the combustion efficiency is adversely affected by both high altitudes and low engine speeds (reference 6), the effect of altitude on corrected fuel flow (and corrected specific fuel consumption) will be even greater than would be expected from consideration of changes in corrected exhaust-gas temperature and air flow, especially at low corrected engine speeds.

Except at low corrected engine speeds, the corrected net thrust increased as altitude was increased at a given corrected engine speed (figs. 4(i) and 4(j)). Even at low corrected engine speeds this trend was evident at altitudes above 50,000 feet. These trends in corrected net thrust, which are similar to those shown in reference 7, are due to changes in corrected air flow, exhaust-gas temperature, and turbine-inlet pressure which are affected by decreased component efficiencies with increased altitude. At lower corrected engine speeds where the change in corrected net thrust with altitude is less (in some cases nonexistent) the decrease in corrected air flow offsets the increase in corrected exhaust-gas temperature and pressure.

Performance Maps

The engine performance maps presented in figure 5 were cross-plotted from data shown in figure 4 and similar data for other exhaust-nozzle areas. A map was constructed for each of the four flight conditions at which data for a full range of exhaust-nozzle areas and engine speeds were obtained. The coordinates of these maps are exhaust-gas temperature and engine speed with lines of constant net thrust, specific fuel consumption, and projected exhaust-nozzle area superimposed. Also shown are lines that indicate the exhaust-gas temperature that gives limiting turbine-inlet bulk and local temperatures. The limiting local turbine-inlet temperature is reached when the temperature at any radial position at the turbine inlet equals the manufacturer's specified limit for that particular radial position (reference 3). Curves shown above this latter limit were extrapolated.

The minimum specific fuel consumption encountered at these four flight conditions was about 1.20 pounds per hour per pound thrust and occurred at an altitude of 35,000 feet and a flight Mach number of 0.62 (fig. 5(c)). At the other flight conditions investigated, the minimum

specific fuel consumption was about 1.25 pounds per hour per pound thrust. At high engine speeds, closing the exhaust nozzle from an area of 421 to 367 square inches resulted, in general, in an increase in specific fuel consumption. This increase is associated with a reduction in compressor efficiency as the compressor pressure ratio is increased (reference 2).

As total pressure at the engine inlet was reduced, the exhaust-gas temperature at which limiting turbine-inlet local temperature occurred approached the exhaust-gas temperature at which limiting turbine-inlet bulk temperature was encountered (fig. 5). As stated in reference 3, this is caused by the closer matching of the turbine-inlet temperature profiles with the manufacturer's specified profile as the engine-inlet total pressure was decreased. If the actual and the recommended profile were identical, the exhaust-gas temperature would, of course, be the same for either turbine-inlet limit. Because of mismatching of these profiles at low altitudes, only about 95 percent of the maximum net thrust possible could be realized without exceeding the local turbine-inlet temperature limit (fig. 5(a)).

In the region above 75 percent of maximum net thrust for any flight condition, no large difference in specific fuel consumption was obtained for any particular schedule of exhaust-nozzle area and engine speed. Therefore, the exhaust-nozzle schedule used is not critical insofar as steady-state performance is concerned. Acceleration and thrust modulation are therefore the determining factors in the manufacturer's selection of an exhaust-nozzle schedule. The steady-state exhaust-nozzle schedule that allows the exhaust nozzle to remain open until rated engine speed is reached appears to give the best transient performance because: (1) the maximum rate of acceleration is possible, and (2) large increases in thrust may be obtained almost instantaneously by closing the exhaust nozzle at any engine speed. For example, at an engine speed of 6500 rpm, an altitude of 15,000 feet, and a flight Mach number of 0.62, it is possible to obtain about 55 percent thrust modulation. Using the previous example as a qualitative, but not quantitative guide, by operating with the exhaust nozzle open at the reduced thrust levels required during a landing approach or cruise condition, a large and almost instantaneous thrust increase is available in case of a "wave-off" or similar maneuver.

Use of Pumping Characteristics and Combustion Efficiency to

Calculate Engine Performance

It is desirable to be able to calculate engine performance at flight conditions other than those presented in this report. In order to do this from pumping characteristics, it is necessary to define the

effect of a change in engine operating and flight condition on several engine parameters. To meet this requirement, the effect of Reynolds number on engine pumping and air-flow characteristics must be determined. It is also necessary that the variation of combustion efficiency and effective velocity coefficient of the exhaust nozzle be defined in terms of engine parameters that are readily available. In the following paragraphs these relations will be discussed and the curves necessary to calculate engine performance will be presented. It is important to note that engine pressure ratio does not include inlet-duct losses. Performance including duct losses may be calculated if these losses are known.

2733
Engine air flow and pressure ratio. - Engine air flow and pressure ratio are shown as functions of engine temperature ratio for constant corrected engine speeds at a Reynolds number index of 0.222 in figures 6(a) and 7(a), respectively. Correction factors which account for the effect of Reynolds number on the air-flow and pumping characteristics are presented in figures 6(b) and 7(b). The correction factor for corrected air flow is the ratio of corrected air flow at the Reynolds number index in question to the corrected air flow at a Reynolds number index of 0.222. Similarly, the correction factor for engine pressure ratio is the ratio of pressure ratio at the Reynolds number index in question to the pressure ratio at a Reynolds number index of 0.222. Selection of the reference Reynolds number index (0.222 in this case) was made in order to utilize the high corrected engine speeds and engine temperature ratios investigated at this Reynolds number index.

Combustion efficiency. - Combustion efficiency is presented as a function of a combustion parameter W_aT_6 in figure 8. The restrictions imposed by the derivation of this parameter, which is given in appendix B, are that the corrected engine speed be about 75 percent of rated speed or greater, and that the engine temperature rise be 700° F or more.

Fuel flow. - With the assumption of unity combustion efficiency, engine temperature rise is plotted as a function of fuel-air ratio with lines of constant engine-inlet air temperature in figure 9 (data from reference 8). The use of this figure in conjunction with figure 8 makes it possible to calculate an actual fuel-air ratio. All the variables required to obtain fuel flow and ideal thrusts (no tail-pipe or nozzle losses) have been presented in figures 6 through 9.

Effective velocity coefficient. - An effective velocity coefficient given in figure 10 is required to calculate actual values of thrust. An explanation of the parameters used on this figure is given in appendix A.

A sample problem demonstrating the use of figures 6 through 10 is given in appendix C.

Engine Performance Obtained from Pumping Characteristics and Direct Experimental Data

Net thrust and fuel flow for the military and normal engine operating conditions are presented as a function of true airspeed for seven altitudes in figures 11 to 13. The data presented in figure 11 were calculated by means of the pumping characteristics and supplementary curves (figs. 6 to 10). Data presented on figure 12 were obtained from experimental data, using the method described earlier which avoids the necessity of duplicating flight ambient pressure in the tunnel test section. Figure 13 presents both experimental and calculated data. The experimental data shown in figures 12 and 13 were obtained at flight Mach numbers as high as 1.68. For military and normal conditions, the engine speed is 7260 rpm and the exhaust-gas temperatures are 1580° and 1440° R, respectively. These temperatures correspond to turbine-inlet temperatures of 1885° and 1750° R.

These data show that at low flight speeds (fig. 11(a)) the net thrust decreased as flight speed was increased from 0 to about 275 knots. Above flight speeds of about 275 knots (figs. 11 to 13), the net thrust increased with flight speed at an increasing rate up to a flight speed of about 900 knots. Further increase in flight speed resulted in a decrease in the rate at which net thrust increased (figs. 11(d) to 13). This latter trend is associated with the relation of inlet-air temperature to flight speed and the effect of reduced corrected engine speed and engine temperature ratio on the engine pressure ratio. Fuel flow increased with flight speed over the entire range of flight speeds.

A comparison of experimental data and data calculated from pumping characteristics is possible at an altitude of 60,000 feet (fig. 13). For the curves showing military operation, the maximum discrepancy in both net thrust and fuel flow is about 2 percent at high flight speeds. The curves showing normal operation are not in as close agreement, the maximum difference being about 4 percent at high flight speeds.

SUMMARY OF RESULTS

Fixed-exhaust-nozzle performance data were obtained at altitudes as high as 55,000 feet and flight Mach numbers as high as 0.99. In general, increasing the altitude resulted in an increase in corrected net thrust at a given corrected engine speed. Above a corrected engine speed of 7000 rpm, changing altitude at a given corrected engine speed had no

effect on corrected air flow. However, below a corrected engine speed of 7000 rpm, the corrected air flow decreased as altitude was increased at a given corrected engine speed. For the four flight conditions at which engine performance maps were obtained, the minimum specific fuel consumption was about 1.20 pounds per hour per pound of thrust and occurred at an altitude of 35,000 feet and a flight Mach number of 0.62. The effect of exhaust-nozzle area and engine speed on specific fuel consumption was small at thrust levels above 75 percent of maximum. The selection of a schedule of exhaust-nozzle area and engine speed is therefore primarily dependent on the consideration of the acceleration characteristics.

A method is presented to define the effect that a change in engine operating and flight condition would have on engine-pumping and air-flow characteristics, and combustion efficiency. This permits the calculation of net thrust and fuel flow for conditions at which data points were not obtained. These calculated values agreed closely with the actual values obtained. Curves of thrust and fuel flow for both military and normal operating conditions are shown for altitudes from 15,000 to 60,000 feet and flight speeds of zero to 1100 knots.

Lewis Flight Propulsion Laboratory
National Advisory Committee for Aeronautics
Cleveland, Ohio

APPENDIX A

SYMBOLS AND METHODS OF CALCULATION

Symbols

The following symbols are used in this report:

A	cross-sectional area, sq ft
B	thrust scale reading, lb
C _v	effective velocity coefficient, ratio of scale jet thrust to rake jet thrust calculated at turbine outlet
D	external drag of installation, lb
F _j	jet thrust, lb
F _n	net thrust, lb
g	acceleration due to gravity, 32.2 ft/sec ²
K	constant
M	Mach number
N	engine speed, rpm
P	total pressure, lb/sq ft abs
p	static pressure, lb/sq ft abs
R	gas constant, 53.4 ft-lb/(lb)(°R)
T	total temperature, °R
t	static temperature, °R
V	velocity, ft/sec or knots
W _a	air flow, lb/sec
W _g	gas flow, lb/sec
W _f	fuel flow, lb/hr
γ	ratio of specific heats

δ ratio of engine-inlet absolute total pressure to absolute static pressure of NACA standard atmosphere at sea level

η_b combustion efficiency

ρ density, slugs/cu ft

θ ratio of engine-inlet absolute total temperature to absolute static temperature of NACA standard atmosphere at sea level

φ ratio of absolute viscosity of air at the engine inlet to the absolute viscosity of NACA standard atmosphere at sea level

$\frac{\delta}{\varphi \sqrt{\theta}}$ Reynolds number index

Subscripts:

e equivalent

eff effective

i indicated

r rake

s scale

0 free stream

1 inlet duct

2 engine inlet

3 compressor inlet

4 compressor outlet or combustor inlet

5 combustor outlet or turbine inlet

6 turbine outlet

7 exhaust-nozzle inlet

Method of Calculations

Flight Mach number. - The flight Mach number, when complete ram-pressure recovery was assumed, was calculated from the expression

$$M_0 = \sqrt{\frac{2}{\gamma_2 - 1} \left[\left(\frac{P_2}{P_0} \right)^{\frac{\gamma_2}{\gamma_2 - 1}} - 1 \right]} \quad (1)$$
2733

Airspeed. - The following equation was used to calculate airspeed:

$$v_0 = M_0 \sqrt{\gamma g R T_2 \left(\frac{P_0}{P_2} \right)^{\frac{\gamma_2}{\gamma_2 - 1}}} \quad (2)$$

Temperature. - Total temperatures were determined from indicated temperatures by the following relation:

$$T = \frac{T_1 \left(\frac{P}{P_1} \right)^{\frac{\gamma-1}{\gamma}}}{1 + 0.85 \left[\left(\frac{P}{P_1} \right)^{\frac{\gamma-1}{\gamma}} - 1 \right]} \quad (3)$$

where 0.85 is the impact recovery factor for the type of thermocouple used.

Air flow. - The air flow was determined from pressure and temperature measurements by the following equation:

$$w_{a,1} = p_1 A_1 \sqrt{\frac{2 \gamma_1 g}{(\gamma_1 - 1) R t_1} \left[\left(\frac{P_1}{P_0} \right)^{\frac{\gamma_1 - 1}{\gamma_1}} - 1 \right]} \quad (4)$$

Gas flow. - The gas flow downstream of the combustor was calculated as follows:

$$W_{g,5} = W_{a,1} + \frac{W_f}{3600} \quad (5)$$

Scale thrust. - Values of thrust based on scale measurements were found for both the data with fixed-exhaust-nozzle areas and control-scheduled data. The jet thrust of the installation was determined from the balance-scale measurements by using the following equation:

$$F_{j,s} = B + D + \frac{W_{a,1} V_1}{g} + A_1(p_1 - p_0) \quad (6)$$

When a tail rake was installed, the drag of the rake was added to the right side of the equation. The last two terms of this expression represent the momentum and pressure forces on the installation at the slip joint in the inlet-air duct. The external drag of the installation was determined with the engine inoperative.

Scale net thrust was obtained by subtracting the free-stream momentum of the inlet air from the scale jet thrust:

$$F_{n,s} = F_{j,s} - \frac{W_{a,1} V_0}{g} \quad (7)$$

Calculated thrust. - For the data shown in figures 11 through 13, thrust was calculated from conditions at the turbine outlet. For the experimental data, turbine-outlet conditions were measured; while, for data calculated from pumping characteristics, the turbine-outlet conditions were predicted from data at other flight conditions.

Ideal jet thrust was calculated from conditions at the turbine outlet by the following equation:

$$F_{j,r} = \frac{W_{g,6}}{g} V_{eff} \quad (8)$$

In a perfect converging exhaust nozzle,

$$V_{eff} = V_n + \frac{A_n(p_n - p_0)}{\frac{W_{g,6}}{g}} \quad (9)$$

where V_n , A_n , and p_n are the velocity, the area, and the static pressure at the vena contracta. The term $V_{eff}/\sqrt{gRT_6}$ is called the effective velocity parameter and is a function of the exhaust-nozzle pressure ratio and specific heat ratio, as given in figure 14. A further discussion of the effective velocity concept is given in reference 9.

The thrust calculated by equation (8) is an ideal thrust in that it does not include total-pressure losses in the tail pipe and the exhaust nozzle. These losses may most easily be considered by means of an effective velocity coefficient (fig. 10), which is defined as the ratio of scale jet thrust to jet thrust calculated at turbine-outlet conditions. The effective velocity coefficient was obtained from the data given in tables I and II and was found to be primarily a function of turbine-outlet Mach number. Inasmuch as it is impractical to calculate turbine-outlet Mach number by means of a static pressure, a more practical means was used. From continuity considerations

$$\frac{W_{g,6}\sqrt{T_6}}{KP_6} = f(M_6) \quad (10)$$

where K is a constant equal to the effective flow area at the turbine outlet. In the data presented in figure 10, in which effective velocity coefficient C_v is shown as a function of turbine-outlet gas-flow parameter $W_{g,6}\sqrt{T_6}/P_6$ the constant K has been included in the values of the gas-flow parameter on the abscissa.

For the data for which calculated rather than scale values of thrust were used, the exhaust-nozzle pressure ratios p_0/p_6 may be below the limit imposed by the tunnel equipment. However, effective velocity coefficients based on a convergent nozzle are only slightly affected at exhaust-nozzle pressure ratios below critical.

APPENDIX B

DERIVATION OF COMBUSTION PARAMETER, $W_a T_6$

If the turbine nozzles are assumed choked,

$$\frac{W_g \sqrt{T_5}}{P_5} = K_1 \quad (11)$$

Experimental results from various engines show that in the range of operation where the turbine nozzles are choked the following relation is valid:

$$T_5 \approx K_2 T_6 \quad (12)$$

Combining the two equations yields

$$\frac{W_g \sqrt{T_6}}{P_5} \approx \frac{K_1}{\sqrt{K_2}} \quad (13)$$

Since $W_g \approx W_a$ and $P_5 \approx P_4$

$$\frac{W_a \sqrt{T_6}}{P_4} \approx \frac{K_1}{\sqrt{K_2}} \quad (14)$$

or

$$P_4 \approx \frac{\sqrt{K_2} W_a \sqrt{T_6}}{K_1} \quad (15)$$

Because the Mach numbers are low at the combustor inlet ($M < 0.2$), the total temperature and pressure can be used with little error in place of the static temperature and pressure so that

$$\rho_4 = \frac{P_4}{g R T_4} \quad (16)$$

and

$$V_4 = \frac{W_a R T_4}{P_4 A_4} \quad (17)$$

Substituting equations (15) and (17) for pressure and velocity, respectively, in $P_4 T_4 / V_4$ yields the following equation:

$$\frac{P_4 T_4}{V_4} \approx \frac{K_2 A_4 W_a T_6}{K_1^2 R} \quad (18)$$

The parameter $P_4 T_4 / V_4$ has often been used to correlate combustion efficiency. Because all the terms in the right side of equation (17) are constants except $W_a T_6$, it may be used in place of $P_4 T_4 / V_4$ to correlate combustion efficiency.

APPENDIX C

SAMPLE PROBLEM

The thrust and the fuel flow are calculated for the conditions of run 54 of table II. The following quantities are known:

$$P_0 = 222 \text{ lb/sq ft} \quad T_6 = 1532^\circ \text{ R}$$

$$P_2 = 288 \text{ lb/sq ft} \quad N = 7260 \text{ rpm}$$

$$T_2 = 435^\circ \text{ R}$$

From these quantities the following parameters may be calculated:

$$N/\sqrt{\theta} = 7934 \text{ rpm} \quad \sqrt{\theta} = 0.915$$

$$T_6/T_2 = 3.50 \quad \delta/\varphi\sqrt{\theta} = 0.168$$

$$\delta = 0.1361 \quad V_0 = 610 \text{ ft/sec}$$

$$\theta = 0.838$$

From figures 6(a) and 7(a),

$$\left(\frac{P_6}{P_2}\right)_{\delta/\varphi\sqrt{\theta}} = 0.222 = 2.130$$

$$\left(\frac{W_a\sqrt{\theta}}{\delta}\right)_{\delta/\varphi\sqrt{\theta}} = 0.222 = 148.2 \text{ lb/sec}$$

From figures 6(b) and 7(b),

Correction factor for pressure ratio = 0.992

Correction factor for corrected air flow = 1.000

Therefore

$$\left(\frac{P_6}{P_2}\right)_{\delta/\varphi\sqrt{\theta}} = 0.168 = 2.113$$

$$\left(\frac{W_a\sqrt{\theta}}{\delta}\right)_{\delta/\varphi\sqrt{\theta}} = 0.168 = 148.2 \text{ lb/sec}$$

$$(W_a)_{\delta/\varphi\sqrt{\theta}} = 0.168 = 22.04 \text{ lb/sec}$$

$$(P_6)_{\delta/\varphi\sqrt{\theta}} = 0.168 = 609 \text{ lb/sq ft}$$

In order to calculate fuel flow and thereby obtain gas flow, the following steps are required:

$$W_a T_6 = (22.04)(1532) = 3.38 \times 10^4 \text{ (lb)(}^{\circ}\text{R)}/\text{sec}$$

From figure 8,

$$\eta_b = 0.928$$

The engine temperature rise is

$$T_6 - T_2 = 1097^{\circ} \text{ R}$$

From figure 9,

$$(W_f/3600 W_a)_{\text{ideal}} = 0.0152$$

The actual fuel-air ratio is

$$(W_f/3600 W_a)_{\text{actual}} = \frac{0.0152}{0.928} = 0.0164$$

The gas flow is

$$\begin{aligned} W_{g,6} &= W_a [1 + (W_f/3600 W_a)_{\text{actual}}] \\ &= (22.04)(1.0164) \\ &= 22.40 \text{ lb/sec} \end{aligned}$$

The next steps in the calculation of thrust are as follows:

$$p_0/P_6 = 222/609$$

$$= 0.365$$

$$\gamma = 1.336 \text{ for a } W_f/3600 W_a \text{ of 0.0164 and a } T_6 \text{ of } 1532^{\circ} \text{ R}$$

From figure 14,

$$\frac{V_{\text{eff}}}{\sqrt{gRT_6}} = 1.328$$

and

$$\begin{aligned} V_{\text{eff}} &= 1.328 \sqrt{(32.2)(53.4)(1532)} \\ &= 2155 \text{ ft/sec} \end{aligned}$$

The ideal or rake jet thrust is

$$\begin{aligned} F_{j,r} &= (w_{g,6}/g) V_{\text{eff}} \\ &= \frac{22.40}{32.2} (2155) \\ &= 1499 \text{ lb} \end{aligned}$$

The inlet momentum is

$$\begin{aligned} \left(\frac{w_{a,1}}{g}\right) v_0 &= \frac{22.04}{32.2} (610) \\ &= 418 \text{ lb} \end{aligned}$$

The ideal or rake net thrust is

$$\begin{aligned} F_{n,r} &= F_{j,r} - \frac{w_{a,1}v_0}{g} \\ &= 1499 - 418 \\ &= 1082 \text{ lb} \end{aligned}$$

The fuel flow is

$$\begin{aligned} w_f &= 3600 w_{a,1} \left[\left(\frac{w_f}{3600 w_{a,1}} \right)_{\text{actual}} \right] \\ &= (3600)(22.04)(0.0164) \\ &= 1301 \text{ lb/hr} \end{aligned}$$

Values of calculated ideal net thrust and fuel flow are 1082 pounds and 1301 pounds per hour, respectively. The values from the data are 1087 pounds and 1292 pounds per hour. Therefore, the calculated values are 0.37 percent low for ideal net thrust and 0.70 percent high for fuel flow.

In order to calculate an actual or more realistic thrust, it is necessary to obtain an effective velocity coefficient. The following steps are required:

$$\frac{W_{g,6}\sqrt{T_6}}{P_6} = \frac{22.40\sqrt{1532}}{609} = 1.439$$

Using this value and figure 10,

$$C_v = 0.940$$

The actual jet thrust is

$$\begin{aligned} (F_j)_{\text{actual}} &= C_v (F_{j,r}) \\ &= (0.940)(1499) \\ &= 1409 \text{ lb} \end{aligned}$$

The actual net thrust is

$$\begin{aligned} (F_n)_{\text{actual}} &= (F_j)_{\text{actual}} - \frac{W_{a,1}V_0}{g} \\ &= 1409 - 418 \\ &= 991 \text{ lb} \end{aligned}$$

The specific fuel consumption is

$$W_f/F_n = \frac{1301}{991} = 1.313$$

It should be noted that for any engine condition for which the performance may be desired, the corresponding engine speed and exhaust-gas temperature must be within the physical capabilities of the exhaust nozzle. This can be verified by the data of figure 5.

2733
REFERENCES

1. Finger, Harold B., Essig, Robert H., and Conrad, E. William: Effect of Rotor- and Stator-Blade Modifications on Surge Performance of an 11-Stage Axial-Flow Compressor. I - Original Production Compressor of XJ40-WE-6 Engine. NACA RM SE52G03.
2. Conrad, E. William, Finger, Harold B., and Essig, Robert H.: Effect of Rotor- and Stator-Blade Modifications on Surge Performance of an 11-Stage Axial-Flow Compressor. II - Redesigned Compressor for XJ40-WE-6 Engine. NACA RM E52I10.
3. Prince, W. R., and Schulze, F. W.: Altitude Investigation of Gas Temperature Distribution at Turbine of Three Similar Axial-Flow Turbojet Engines. NACA RM E52H06.
4. Sanders, Newell D., and Behun, Michael: Generalization of Turbojet-Engine Performance in Terms of Pumping Characteristics. NACA TN 1927, 1949.
5. Sanders, Newell D.: Performance Parameters for Jet-Propulsion Engines. NACA TN 1106, 1946.
6. Sobolewski, Adam E., Miller, Robert R., and McAulay, John E.: Altitude Performance Investigation of Two Single-Annular Type Combustors and the Prototype J40-WE-8 Turbojet Engine Combustor with Various Combustor-Inlet Air Pressure Profiles. NACA RM E52J07.
7. Fleming, William A.: Effects of Altitude on Turbojet Engine Performance. NACA RM E51J15, 1951.
8. Turner, L. Richard, and Bogart, Donald: Constant-Pressure Combustion Charts Including Effects of Diluent Addition. NACA Rep. 937, 1949. (Supersedes NACA TN's 1655 and 1086.)
9. Turner, L. Richard, Addie, Albert N., and Zimmerman, Richard H.: Charts for the Analysis of One-Dimensional Steady Compressible Flow. NACA TN 1419, 1948.

TABLE I. - FIXED-

Run	Altitude (ft)	Ram pressure ratio P_1/P_0	Flight Mach number M_0	Tunnel static pressure P_0 (lb/sq ft abs)	Reynolds number $\theta_0/2\sqrt{R_2}$	Equivalent ambient-air temperature $\theta_{a,e}$ (°R)	Engine-inlet temperature T_2 (°R)	Actual engine speed N (rpm)	Corrected engine speed $N/\sqrt{R_2}$ (rpm)	Ideal net thrust $F_{n,r}$ (lb)	Actual net thrust $F_{n,s}$ (lb)	Corrected ideal jet thrust $F_{n,r}/\theta_0$ (lb)	Ideal jet thrust $F_{j,r}$ (lb)
Exhaust-nozzle													
1	15,000	1.299	0.622	1187	0.758	464	500	6534	6658	4001	3748	5151	5882
2		1.301	.625	1184	.756	465	501	6553	6687	3511	3255	4472	5315
3		1.298	.621	1183	.754	464	500	6171	6288	3059	2827	3901	4762
4		1.298	.622	1186	.757	464	500	5908	5918	2298	2038	2800	3845
5		1.298	.615	1190	.754	465	500	5082	5179	1100	997	1577	2322
6	35,000	1.303	0.627	479	0.358	413	445	6171	6668	1691	1575	5332	2439
7		1.303	.627	479	.358	413	446	5980	6463	1487	1363	4621	2201
8		1.294	.628	477	.355	413	448	5908	6267	1279	1218	4142	1952
9		1.299	.625	478	.354	414	446	5445	5875	925	855	2914	1821
10		1.296	.621	479	.354	414	446	5082	5483	656	588	1935	1185
11		1.673	.992	478	.462	390	467	6534	6887	2677	2436	5781	4414
12		1.873	.992	473	.484	386	463	6553	6726	2568	—	4018	—
13		1.869	.990	479	.488	389	465	6171	6517	2051	—	5858	—
14		1.872	.991	478	.479	385	470	5808	6104	1457	1313	3104	2682
15		1.863	.987	481	.480	385	469	5082	5348	615	495	1164	1802
16	45,000	1.295	0.618	288	0.221	404	435	5980	6541	983	884	5018	1377
17		1.327	.649	286	.224	402	436	5808	6537	840	795	4420	1257
18		1.311	.634	288	.222	404	437	5445	5835	610	587	3176	878
19		1.313	.636	288	.222	405	438	5082	5534	428	371	2069	761
Exhaust-nozzle													
20	15,000	1.292	0.618	1186	0.747	468	504	7260	7389	4645	4382	6052	6761
21		1.281	.616	1184	.746	468	503	7079	7192	4304	4114	5684	6386
22		1.292	.616	1188	.748	467	503	6887	7007	3546	3757	5181	5874
23		1.295	.619	1188	—	—	504	6716	6817	—	—	—	—
24		1.295	.619	1185	.747	467	505	6534	6839	3139	2888	4786	5029
25		1.295	.618	1179	.746	467	503	6171	6270	2363	2264	3136	4085
26		1.291	.616	1185	.742	469	505	5808	6889	1708	1813	2251	3261
27		1.295	.619	1184	.744	469	505	5082	5153	751	662	914	2015
28	35,000	1.303	0.627	479	0.380	411	445	7260	7863	2265	2133	7229	3180
29		1.297	.621	478	.358	412	444	7078	7682	2160	2051	6884	3056
30		1.297	.621	478	.358	412	444	6887	7456	1989	1951	8857	2852
31		1.295	.619	479	.358	412	444	6716	7280	1875	1782	5084	2781
32		1.302	.626	479	.359	412	444	6534	6863	1715	1671	5262	2211
33		1.300	.624	479	.358	413	445	6171	6868	1353	1271	4319	2106
34		1.298	.622	478	.357	413	445	5808	6268	973	905	3087	1667
35		1.302	.626	479	.358	413	445	5012	5489	459	407	1381	1017
36		1.852	.982	461	.479	584	470	7260	7830	2809	2724	8472	4835
37		1.867	.989	479	.482	581	471	7079	7461	2783	2580	6104	4703
38		1.850	.981	478	.476	582	467	6887	7269	2542	2392	5724	4398
39		1.855	.988	479	.478	585	472	6716	7045	2291	2124	5030	4106
40		1.861	.981	471	.471	400	478	6534	6908	1997	1928	4567	3736
41		1.861	.986	478	.478	584	471	6171	6480	1522	1378	3278	5144
42		1.863	.987	480	.480	585	469	5808	6110	1048	875	2071	2555
43		1.850	.981	481	.479	584	470	5082	5341	510	205	487	1802
44	45,000	1.287	0.612	290	0.226	407	437	7079	7716	1385	1318	7479	1914
45		1.290	.614	281	.225	405	437	6887	7518	1537	1256	7078	1688
46		1.289	.614	289	.222	406	436	6716	7327	1557	1158	6470	1224
47		1.299	.623	287	.222	405	436	6534	7129	1112	1047	5943	1619
48		1.291	.616	289	.222	405	436	6171	6735	875	801	4542	1334
49		1.501	.625	288	.224	403	435	5808	6342	635	601	3393	1058
50		1.289	.614	287	.222	405	435	5082	5550	314	274	1768	640
Exhaust-nozzle													
51	15,000	1.284	0.619	1186	0.758	468	502	7260	7383	4076	3870	5057	6216
52		1.288	.614	1191	.752	465	500	7079	7214	3804	3580	4927	5996
53		1.289	.614	1191	.750	460	485	6887	7053	3511	3178	4582	5530
54		1.298	.613	1184	.744	471	506	6716	6803	3110	2839	3908	5084
55		1.292	.624	1188	.751	467	502	6534	6845	2822	2583	3562	4728
56		1.290	.624	1182	.753	466	502	6171	6276	2035	1852	2524	3785
57		1.295	.618	1187	.755	475	511	5808	6564	1429	1219	1879	2989
58		1.501	.625	1187	.745	470	507	5082	5145	528	408	557	1812
59	35,000	1.288	0.622	480	0.358	414	446	7260	7834	2020	1815	6167	2926
60		1.286	.611	484	.355	419	450	7079	7803	1824	1761	5887	2803
61		1.299	.627	482	.353	419	452	6887	7587	1784	1647	5800	2854
62		1.302	.627	480	.356	418	451	6716	7208	1688	1451	4910	2523
63		1.292	.616	481	.353	421	453	6534	6989	1484	1305	4444	2306
64		1.294	.619	480	.353	421	453	6171	6809	1152	1026	3485	1909
65		1.303	.627	479	.352	421	454	5808	6209	824	757	2498	1619
66		1.297	.621	479	.350	422	455	5082	5428	661	294	1001	808
67		1.865	.988	477	.477	593	470	7260	7830	2551	2327	5834	4484
68		1.857	.984	478	.478	584	470	7074	7440	2356	2234	5526	4277
69		1.870	.990	477	.477	595	472	6887	7235	2648	2437	4902	3834
70		1.853	.982	477	.475	596	472	6716	7045	2035	1827	4374	3572
71		1.873	.992	479	.478	584	472	6534	6854	1787	1580	5726	3572
72		1.873	.992	478	.477	584	471	5808	6095	849	708	1678	2336
73		1.868	.989	478	.477	595	472	5082	5336	197	107	265	1392
74		1.854	.983	478	.476	595	471	5082	5336	—	—	—	—
75	45,000	1.289	0.614	280	0.215	416	447	7260	7819	1269	1218	6894	1826
76		1.296	.621	289	.213	415	447	7079	7744	1240	1140	6440	1780
77		1.288	.613	290	.214	413	444	6887	7456	1151	1083	6024	1885
78		1.293	.608	289	.212	414	445	6716	7286	1078	963	5498	1586
79		1.303	.627	280	.213	409	441	6534	7089	982	903	5055	1485
80		1.288	.615	289	.216	410	442	5908	6298	582	510	2895	980
81		1.299	.623	287	.217	407	440	5082	5519	260	224	1265	598

NACA

EXHAUST-NOZZLE DATA

Actual jet thrust $F_{j,s}$ (lb)	Corrected jet thrust F_j/F_2 (lb)	Actual air flow $W_{a,l}$ (lb/sec)	Corrected air flow $W_a/F_2\sqrt{F_2}$ (lb/sec)	Actual fuel flow W_f (lb/hr)	Corrected fuel flow $W_f/F_2\sqrt{F_2}$ (lb/hr)	Actual specific fuel consumption $W_f/W_{a,s}$ (lb/hr) (lb thrust)	Corrected specific fuel consumption $W_f/F_{a,s}\sqrt{F_2}$ (lb)/(hr) (lb thrust)	Actual exhaust-gas temperature T_g (°R)	Corrected exhaust-gas temperature T_g/F_2 (°R)	Engine total- pressure ratio F_5/F_2	Engine total- temperature ratio T_5/T_2	Run
<i>area, 387 sq in.</i>												
5650	7.736	92.15	124.31	4975	6,986	1.327	1.352	1529	1587	1.870	3.058	1
5059	6,951	87.82	118.56	4405	6,161	1.353	1.376	1472	1525	1.749	2.938	2
4530	6,251	83.62	113.22	3910	5,498	1.363	1.409	1408	1462	1.644	2.816	3
3585	4,829	75.89	102.45	3095	4,337	1.520	1.549	1302	1351	1.464	2.604	4
2219	3,084	60.71	82.26	1884	2,652	1.890	1.926	1111	1153	1.176	2.222	5
2321	7,868	58.51	120.88	2070	7,580	1.516	1.421	1476	1721	1.916	3.317	6
2077	7,041	56.78	115.80	1861	6,807	1.565	1.473	1416	1648	1.785	3.175	7
1891	6,431	54.80	109.09	1659	6,088	1.382	1.470	1354	1576	1.676	3.036	8
1451	4,845	50.85	97.46	1300	4,781	1.520	1.641	1242	1446	1.466	2.785	9
1107	5,777	28.00	88.42	1032	3,795	1.817	1.961	1133	1319	1.300	2.540	10
4173	8,989	58.25	131.08	3205	6,016	1.316	1.387	1547	1719	1.995	3.313	11
---	---	55.63	125.55	2840	7,186	---	---	1484	1641	1.878	3.182	12
2784	6,510	48.14	108.32	1850	4,896	1.409	1.481	1227	1358	1.751	2.591	13
1680	3,986	39.82	89.36	991	2,465	2.010	2.118	951	1055	2.611	2.028	14
1298	7,584	21.81	115.28	1315	6,146	1.488	1.624	1525	1818	1.869	3.506	15
1210	6,745	21.01	107.34	1173	7,135	1.479	1.614	1435	1708	1.753	3.291	16
935	5,258	18.96	97.45	942	5,755	1.661	1.611	1303	1548	1.486	2.982	17
704	3,828	17.06	87.38	779	4,728	2.100	2.286	1180	1399	1.325	2.694	18
<i>area, 421 sq in.</i>												
6516	9,001	105.12	145.07	5530	7,752	1.262	1.281	1527	1575	1.835	3.030	20
6188	8,875	102.58	139.82	5150	7,241	1.282	1.272	1474	1521	1.872	2.930	21
5785	7,978	99.94	135.72	4710	6,599	1.254	1.274	1424	1470	1.791	2.851	22
4878	6,737	92.70	126.07	3880	5,416	1.292	1.315	1321	1383	1.820	2.626	24
5988	6,521	84.44	115.18	3080	4,334	1.360	1.382	1219	1258	1.454	2.423	25
5185	4,377	76.41	104.22	2440	3,422	1.513	1.534	1133	1165	1.304	2.244	26
1828	2,858	81.90	84.25	1593	2,229	2,406	2,440	990	1018	1.063	1.950	27
5048	10,350	47.24	147.91	2805	9,580	1.221	1.323	1530	1795	2.114	3.454	28
2847	10,055	48.55	146.90	2450	9,016	1.195	1.291	1483	1734	2.069	3.340	29
2814	5,801	44.94	141.83	2275	8,590	1.168	1.260	1428	1689	2.008	3.216	30
2639	9,004	44.69	141.04	2115	7,800	1.186	1.282	1383	1617	1.935	3.115	31
2421	8,217	45.68	137.11	1935	7,100	1.229	1.328	1331	1586	1.851	2.998	32
2044	6,846	40.03	125.97	1580	5,797	1.243	1.342	1220	1423	1.654	2.742	33
1599	5,454	56.04	115.85	1250	4,605	1.381	1.492	1122	1308	1.454	2.521	34
985	5,275	26.79	90.49	855	3,133	2,101	2,268	979	1142	1.184	2.200	35
4850	11,048	64.86	146.59	3425	6,554	1.257	1.322	1507	1685	2.009	3.206	36
4245	10,647	64.47	144.67	3203	7,982	1.242	1.309	1467	1630	1.953	3.141	37
3245	10,158	62.66	142.19	2950	7,440	1.235	1.300	1410	1567	1.889	3.019	38
3938	9,328	60.70	137.08	2670	6,653	1.267	1.313	1358	1414	1.747	2.877	39
3867	8,887	57.99	131.87	2595	5,915	1.242	1.295	1301	1413	1.659	2.722	40
3000	7,127	54.38	123.25	1855	4,634	1.346	1.414	1177	1285	1.486	2.435	41
2361	5,588	49.84	112.14	1413	3,617	1.615	1.693	1030	1140	1.267	2.196	42
1397	5,322	40.19	95.85	767	3,137	3,741	3,832	815	901	0.959	1.734	43
1850	10,490	28.24	146.93	1650	10,200	1.251	1.364	1551	1845	2.146	3.549	44
1787	10,070	28.13	145.46	1570	9,841	1.250	1.362	1515	1600	2.101	3.457	45
1705	9,825	---	141.40	1420	8,100	1.255	1.362	1428	1528	2.037	3.330	46
1554	25.55	156.01	148.00	8,120	6,169	1.174	1.284	1381	1543	1.857	3.167	47
1230	7,444	24.30	126.29	1085	5,776	1.367	1.492	1278	1521	1.728	2.931	48
1021	8,765	21.92	113.50	895	5,516	1.489	1.636	1171	1396	1.502	2.692	49
600	3,453	17.33	90.77	683	4,269	2,493	2,723	1028	1227	1.206	2.366	50
<i>area, 448 sq in.</i>												
5810	8,006	105.21	142.56	4880	6,559	1.275	1.297	1383	1440	1.754	2.775	51
5552	7,822	105.79	140.95	4470	6,304	1.258	1.279	1386	1418	1.723	2.732	52
5197	7,167	100.86	135.59	4045	5,712	1.275	1.305	1321	1386	1.630	2.669	53
4783	6,595	95.45	131.05	3700	5,157	1.303	1.320	1270	1303	1.567	2.510	54
4489	6,180	94.06	127.55	3410	4,782	1.320	1.345	1222	1284	1.508	2.434	55
3582	4,956	85.29	115.57	2860	3,727	1.452	1.477	1129	1187	1.342	2.248	56
2789	5,840	76.37	104.32	2140	2,970	1.756	1.789	1075	1090	1.215	2.100	57
1892	2,320	62.26	84.36	1580	1,866	3,350	3,589	954	956	1.018	1.842	58
2721	9,248	46.97	147.96	2310	8,458	1.273	1.373	1389	1626	1.932	3.137	59
2840	6,976	46.15	146.11	2115	7,725	1.201	1.290	1374	1584	1.868	3.053	60
2517	8,558	44.73	141.93	1990	7,245	1.208	1.294	1340	1557	1.828	2.965	61
2316	7,837	44.32	159.85	1825	6,626	1.258	1.349	1280	1473	1.764	2.838	62
2126	7,259	42.59	135.48	1681	6,129	1.288	1.378	1240	1422	1.675	2.737	63
1783	6,073	39.20	124.73	1385	5,051	1.350	1.445	1142	1310	1.510	2.521	64
1432	4,854	35.50	112.57	1105	4,004	1.499	1.602	1055	1244	1.355	2.393	65
841	2,864	28.15	89.71	755	2,758	2,561	2,735	916	1045	1.099	2.013	66
4270	10,154	65.11	147.54	2840	7,346	1.263	1.328	1371	1515	1.816	2.817	67
4105	5,766	62.90	142.72	2100	6,566	1.226	1.289	1235	1462	2.115	2.615	68
3638	8,709	60.86	138.94	2100	5,777	1.259	1.321	1239	1363	1.653	2.625	70
3365	7,935	59.52	133.86	2050	5,070	1.297	1.361	1171	1288	1.557	2.481	71
2776	6,560	54.81	123.38	1870	3,897	1.384	1.454	1054	1165	1.346	2.242	72
2198	5,202	49.65	112.21	1200	2,984	1.695	1.776	957	1031	1.171	1.985	73
1303	3,101	40.17	91.15	680	1,701	6,355	6,675	755	831	0.899	1.593	74
1755	9,835	26.26	148.48	1520	8,267	1.250	1.346	1471	1706	1.933	3.281	75
1680	9,480	28.04	147.01	1450	8,624	1.272	1.370	1430	1659	1.965	3.199	76
1587	8,984	27.64	144.86	1350	8,268	1.270	1.373	1371	1603	1.899	3.088	77
1471	8,385	26.86	142.48	1245	7,676	1.293	1.397	1325	1546	1.857	2.976	78
1416	7,927	26.56	137.05	1152	6,998	1.276	1.364	1267	1491	1.741	2.873	79
1128	6,401	24.42	126.11	950	5,856	1,431	1,551	1174	1379	1.580	2.656	80
928	5,288	21.72	115.79	794	4,888	1,557	1,688	1100	1293	1.390	2.489	81
562	3,149	17.35	69.53	627	3,816	2,799	3,040	953	1124	1.126	2.166	82

NACA

2733

TABLE I. - Concluded.

Run	Altitude (ft)	Raw pressure ratio P_2/P_0	Flight Mach number M_0	Tunnel static pressure P_0 (lb/sq ft abs)	Reynolds number $52^2 \cdot 2^7 \cdot U_2$	Equiv. vent ambient-air temperature $T_{0,a}$ (°R)	Engine- inlet total temperature T_2 (°R)	Actual engine speed N (rpm)	Corrected engine speed $N\sqrt{P_2}$ (rpm)	Ideal net thrust $F_{n,r}$ (lb)	Actual net thrust $F_{n,s}$ (lb)	Corrected net thrust $F_{n,s}/5$ (lb)	Ideal jet thrust $F_{j,r}$ (lb)
Exhaust-nozzle													
83	15,000	1.298	0.622	1163	0.751	466	501	7260	7501	3732	3411	4700	5905
84		1.292	.615	1166	.750	465	500	7079	7214	412	3100	4278	5545
85		1.288	.621	1168	.748	468	504	6897	7000	3125	2808	3555	5195
86		1.293	.619	1167	.747	469	505	6716	6810	2789	2498	3440	4781
87		1.300	.624	1187	.749	468	504	6534	6632	2459	2178	2886	4404
88		1.301	.625	1188	.751	468	505	6171	6257	1734	1528	2093	3506
89		1.294	.618	1184	.743	470	506	5808	5984	1217	1061	1465	2802
90		1.295	.619	1185	.740	473	509	5082	5135	429	520	441	1698
91	35,000	1.307	0.631	474	0.352	411	444	7260	7846	1817	1628	5566	2732
92		1.294	.619	478	.355	412	445	7079	7867	1710	1540	5268	2598
93		1.275	.600	483	.350	420	450	7079	7805	1692	1547	5115	2548
94		1.304	.628	480	.361	411	443	6897	7468	1622	1596	4720	2625
95		1.300	.624	477	.354	417	449	6716	7220	1489	1315	4479	2335
96		1.282	.607	479	.350	418	449	6534	7024	1351	1174	4046	2142
97		1.291	.616	482	.355	417	449	6171	6634	1022	887	3016	1792
98		1.302	.626	480	.359	414	446	5808	6267	761	626	2126	1485
99		1.310	.634	479	.359	414	447	5082	5473	525	242	816	907
100		1.379	.994	477	.482	392	469	7260	7859	2311	2078	4909	4280
101		1.370	.990	478	.478	394	471	7079	7455	2183	1971	4656	4124
102		1.382	.986	477	.480	392	470	6897	7249	2010	1768	4187	3920
103		1.380	.981	479	.473	394	470	6716	7059	1785	1561	5702	3805
104		1.383	.982	477	.470	392	469	6534	6930	1529	1356	3708	3578
105		1.387	.984	478	.478	395	471	6171	6480	1129	946	2228	2185
106		1.386	.989	477	.476	394	471	5808	6098	691	504	1187	1503
107		1.384	.983	478	.477	394	470	5082	5341	96	7	17	1503
108	45,000	1.288	0.615	289	0.210	408	439	7260	7852	1185	1047	5852	1721
109		1.290	.624	291	.214	405	437	7079	7716	1159	1031	5785	1691
110		1.301	.615	289	.204	404	439	6897	7585	1047	944	5344	1457
111		1.285	.610	288	.209	420	451	6716	7208	931	798	4581	1435
112		1.288	.614	291	.213	415	446	6534	7050	855	710	4004	1355
113		1.286	.621	291	.216	410	442	6171	6693	690	585	3282	1162
114		1.296	.621	291	.219	409	440	5808	6307	503	447	2506	925
115		1.300	.624	291	.216	415	447	5082	5473	228	140	783	574
Exhaust-nozzle													
116	15,000	1.297	0.621	1161	0.743	467	505	7260	7376	3212	2656	3670	5368
117		1.294	.619	1185	.751	465	500	7079	7190	2855	2465	3408	5059
118		1.295	.618	1155	.741	469	505	6897	6884	—	2167	2993	—
119		1.295	.618	1153	.739	470	508	6716	6803	2253	1905	2833	4505
120		1.295	.618	1153	.758	472	508	6534	6602	2035	1625	2244	3526
121		1.295	.622	1182	.755	472	509	6171	6285	1443	1168	157	3226
122		1.296	.621	1182	.752	474	510	5808	6680	801	585	1001	2262
123		1.297	.621	1181	.752	474	511	5082	5125	232	150	191	1525
124	35,000	1.293	0.618	479	0.360	409	440	7260	7884	—	1547	4601	—
125		1.285	.619	460	.380	409	440	7079	7888	1559	1274	4357	2435
126		1.293	.616	479	.362	408	439	6897	7447	—	1547	4359	—
127		1.297	.621	479	.365	409	441	6716	7287	1325	1083	3680	2194
128		1.293	.618	481	.369	410	441	6534	7089	—	864	3480	—
129		1.294	.619	481	.358	410	441	6171	6698	952	751	2553	1747
130		1.294	.619	478	.358	411	442	5808	6296	614	490	1643	1328
131		1.288	.622	479	.358	410	442	5082	5509	228	159	541	794
132		1.380	.985	479	.480	392	468	7280	7645	2074	1718	4073	4021
133		1.361	.988	478	.479	392	468	7079	7454	1958	1560	3687	3882
134		1.372	.991	477	.482	391	468	6897	7263	1801	1416	3356	3704
135		1.383	.986	476	.481	391	469	6716	7065	—	1228	2899	—
136		1.374	.992	477	.476	394	472	6534	6854	1368	1045	2470	3159
137		1.384	.997	477	.480	394	472	6171	6473	908	662	1559	2655
138		1.380	.985	476	.478	393	471	5808	6098	536	354	790	2054
139		1.378	.993	478	.479	393	471	5082	5356	-17	-145	-357	1222
140	45,000	1.287	0.612	290	0.210	424	456	7260	7746	992	628	4696	1526
141		1.295	.618	290	.212	420	452	7079	7582	—	795	4485	—
142		1.302	.626	287	.211	417	450	6897	7407	906	697	5946	1443
143		1.294	.619	289	.212	415	447	6716	7233	837	707	3972	1355
144		1.298	.622	290	.215	413	445	6534	7057	768	622	3498	1282
145		1.278	.603	289	.212	414	444	6171	6671	596	492	2619	1054
146		1.285	.619	291	.216	411	443	5908	6290	585	352	1864	907
147		1.300	.624	294	.221	411	443	5082	5504	174	90	498	523
148	50,000	1.284	0.609	224	0.168	405	435	7260	7928	849	716	5266	1266
149		1.286	.591	234	.171	405	433	7079	7752	819	695	4951	1231
150		1.280	.605	225	.150	446	479	6716	6931	586	473	3474	965
151		1.300	.624	222	.182	440	474	6534	6835	499	435	3189	872
152		1.283	.608	226	.147	451	484	5808	6011	250	183	1335	547
153		1.295	.618	225	.147	451	486	5082	5256	84	2	15	323
154	55,000	1.314	0.637	162	0.122	408	441	7079	7681	660	555	5516	984
155		1.315	.658	164	.128	405	438	6716	7314	523	417	4092	838
156		1.304	.628	169	.130	406	438	6534	7118	482	385	3696	785
157		1.295	.619	168	.129	407	438	5808	6325	262	240	2334	507
158		1.279	.604	170	.124	410	440	5082	5519	124	91	885	309



FIXED-EJECTOR-NOZZLE DATA

Actual jet thrust $F_{j,s}$ (lb)	Corrected jet thrust $F_{j,s}/F_2$ (lb)	Actual air flow $W_{a,1}$ (lb/sec)	Corrected air flow $W_{a,1}\sqrt{F_2/F_1}$ (lb/sec)	Actual fuel flow W_f (lb/hr)	Corrected fuel flow $W_f/F_2\sqrt{F_2/F_1}$ (lb/hr)	Actual specific fuel consumption $W_f/W_{a,s}$ (lb)/(hr)	Corrected specific fuel consumption $W_f/W_{a,s}\sqrt{F_2/F_1}$ (lb)/(hr)	Actual exhaust-gas temperature T_e ($^{\circ}$ K)	Corrected exhaust-gas temperature T_e/F_2 ($^{\circ}$ R)	Engine total-pressure ratio P_g/F_2	Engine total-temperature ratio T_g/F_2	Run
<i>area, 479 sq. in.</i>												
5584	7.695	106.35	145.97	4570	6.131	1.281	1.304	1308	1555	1.659	2.611	53
5203	7.180	103.84	140.60	4030	5.668	1.300	1.322	1259	1307	1.615	2.516	64
4876	6.700	101.22	137.05	3715	5.181	1.324	1.344	1224	1281	1.547	2.429	85
4490	6.183	97.50	132.41	3585	4.698	1.347	1.365	1189	1222	1.481	2.354	86
4125	5.653	94.58	127.78	3553	4.224	1.393	1.415	1145	1179	1.412	2.272	87
3501	4.819	88.56	116.05	2595	3.325	1.566	1.589	1080	1090	1.265	2.099	88
2846	5.584	77.58	105.82	1945	2.721	1.833	1.457	1005	1051	1.162	1.986	89
1589	2.183	61.83	84.40	1287	1.791	4.022	4.063	908	926	1.998	1.784	90
2544	8.893	46.96	146.59	2000	7.588	1.226	1.327	1292	1510	1.812	2.910	91
2428	8.306	46.45	146.83	1882	6.972	1.222	1.325	1248	1464	1.757	2.817	92
2403	8.287	45.71	146.27	1855	6.845	1.199	1.288	1256	1448	1.784	2.791	93
2299	7.773	46.58	145.45	1770	6.481	1.268	1.375	1205	1411	1.708	2.718	94
2179	7.453	44.83	141.81	1620	5.942	1.234	1.327	1172	1355	1.648	2.610	95
1885	6.840	42.88	137.43	1512	5.600	1.288	1.384	1158	1316	1.591	2.535	96
1857	5.854	40.14	126.92	1245	4.549	1.404	1.508	1047	1210	1.428	2.352	97
1512	4.756	37.31	117.92	1050	5.762	1.640	1.769	978	1158	1.368	2.193	98
826	7.785	49.42	99.02	750	2.725	5.089	5.339	894	1002	1.058	2.053	99
4048	9.857	58.69	147.41	2815	6.935	1.288	1.323	1276	1413	1.701	2.721	100
3912	9.240	64.85	145.91	2475	6.159	1.286	1.319	1246	1344	1.649	2.645	101
3678	8.689	65.58	142.81	2255	5.586	1.275	1.340	1194	1319	1.596	2.540	102
3561	8.023	61.02	138.88	2040	5.118	1.315	1.382	1148	1268	1.531	2.443	103
3355	7.954	59.65	134.75	1825	4.572	1.171	1.234	1097	1237	1.450	2.344	104
2578	6.143	54.71	124.19	1435	5.581	1.514	1.580	988	1080	1.274	2.098	105
1996	4.741	49.89	112.85	1049	2.615	2.081	2.185	880	971	1.095	1.868	106
1214	2.899	40.61	92.27	800	1.507	85.71	90.14	723	798	.849	1.538	107
1585	8.011	28.52	149.10	1574	8.493	1.512	1.427	1368	1617	1.855	3.116	108
1581	8.843	28.82	147.90	1510	7.987	1.275	1.388	1515	1562	1.821	5.009	109
1487	8.370	28.33	146.15	1223	7.509	1.296	1.413	1281	1524	1.790	2.958	110
1302	7.442	28.45	140.93	1101	6.751	1.380	1.480	1239	1426	1.688	2.747	111
1210	6.824	28.23	137.13	1020	6.210	1.437	1.551	1185	1377	1.615	2.652	112
1057	5.930	24.85	127.61	887	5.397	1.516	1.644	1105	1296	1.477	2.495	113
869	4.875	22.08	114.07	773	4.707	1.729	1.877	1038	1224	1.320	2.359	114
488	2.719	17.88	92.85	683	5.995	4.738	5.100	842	1083	1.079	2.107	115
<i>area, 555 sq. in.</i>												
4613	6.652	105.44	143.50	3780	5.279	1.416	1.438	1224	1263	1.529	2.453	116
4567	6.318	103.46	140.71	3495	4.910	1.419	1.442	1182	1223	1.483	2.370	117
4215	5.821	100.26	136.54	3200	4.481	1.477	1.497	1145	1177	1.267	2.267	118
3885	5.369	96.80	132.15	2885	4.040	1.514	1.534	1107	1158	1.267	2.188	119
3536	4.883	93.51	127.46	2625	3.685	1.617	1.835	1088	1151	1.100	2.072	120
2841	4.058	86.62	118.52	2040	2.392	1.359	2.379	1035	1025	1.104	1.911	121
2326	3.242	77.76	106.45	1710	2.392	2.359	2.379	985	1085	1.080	1.835	122
1451	1.976	62.73	95.94	1170	1.628	6.476	6.543	843	856	.956	1.050	123
2245	7.658	47.20	146.44	1802	6.685	1.338	1.453	1204	1420	1.736	2.736	124
2170	7.387	46.98	147.24	1860	6.246	1.327	1.440	1174	1444	1.628	2.683	125
2095	7.146	46.42	145.65	1855	5.777	1.339	1.455	1128	1333	1.659	2.659	126
1954	6.655	45.51	142.90	1480	5.470	1.427	1.483	1055	1289	1.536	2.483	127
1805	6.142	44.16	138.53	1560	5.023	1.411	1.551	1048	1251	1.372	2.372	128
1544	5.256	41.66	130.63	1185	4.298	1.531	1.683	992	1168	1.562	2.249	129
1194	4.086	37.34	117.92	915	5.395	1.806	2.087	902	1080	1.205	2.041	130
725	2.467	29.49	92.60	680	2.508	4.277	4.635	805	846	1.018	1.821	131
3682	6.897	65.51	147.75	2350	5.826	1.359	1.430	1205	1356	1.581	2.375	132
3478	6.269	64.78	146.23	2190	5.486	1.413	1.488	1164	1291	1.550	2.487	133
3319	7.866	63.77	145.55	2030	5.067	1.434	1.510	1122	1244	1.497	2.397	134
3089	7.293	62.05	139.20	1480	4.507	1.478	1.585	1055	1188	1.249	2.249	135
2834	6.711	59.70	134.80	1640	4.073	1.572	1.649	1021	1123	1.347	2.163	136
2519	5.461	55.00	125.53	1245	3.078	1.881	1.973	912	1032	1.122	1.992	137
1852	4.378	50.51	115.75	789	2.808	2.049	2.194	802	902	1.030	1.757	138
1098	2.587	41.50	92.84	585	1.507	6.511	6.500	766	766	1.454	1.454	139
1362	7.724	27.65	147.92	1200	7.258	1.445	1.546	1265	1440	1.866	2.774	140
1352	7.514	27.34	146.68	1190	6.826	1.421	1.522	1224	1415	1.651	2.610	141
1220	6.955	24.58	115.05	1057	6.125	1.418	1.528	1157	1343	1.521	2.581	143
1156	6.393	24.38	141.87	1000	6.094	1.425	1.534	1158	1343	1.564	2.581	144
950	5.444	26.67	138.87	930	5.645	1.495	1.614	1109	1253	1.512	2.492	144
756	4.244	22.18	115.10	673	4.093	2.027	2.194	937	1089	1.209	2.118	146
439	2.453	18.10	92.62	585	5.511	7.044	7.071	1022	1104	1.034	1.966	147
1133	6.353	22.56	150.57	985	7.995	1.590	1.518	1280	1538	1.755	2.866	148
1105	7.894	22.76	148.51	955	7.458	1.575	1.506	1234	1480	1.712	2.850	149
852	6.258	19.45	157.24	801	6.128	1.693	1.785	1214	1516	1.486	2.534	150
808	5.924	18.75	151.24	750	5.756	1.724	1.809	1147	1255	1.407	2.420	151
480	5.503	18.11	106.44	639	4.977	5.501	5.727	1027	1100	1.159	2.122	152
241	1.751	11.92	85.79	568	4.284	284.0	295.5	951	953	.982	1.918	153
879	8.758	16.53	151.45	654	8.213	1.539	1.670	1337	1574	1.815	3.032	154
752	7.184	16.12	145.32	779	8.532	1.658	2.034	1336	1550	1.847	2.598	155
688	6.805	15.69	138.37	744	7.777	1.932	2.104	1126	1335	1.570	2.571	156
485	4.718	12.85	114.78	655	6.935	2.728	2.971	977	1158	1.275	2.231	157
276	2.685	9.98	89.22	637	6.752	7.000	7.604	924	1089	1.071	2.100	158

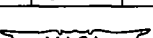


TABLE II. - CONTROL DATA

Run	Altitude (ft)	Res. pressure ratio P_2/P_0	Flight Mach number M_0	Tunnel static pressure P_0 (lb/sq ft abs)	Reynolds number $R_2/\rho_2 V_2$	Equivalent inlet-air temperature T_0 (°R)	Engine- inlet total temperature T_2 (°R)	Engine speed N (rps)	Exhaust- nozzle projected area A_n (sq in.)	Ideal heat thrust $F_{n,i}$ (lb)	Actual heat thrust $F_{n,a}$ (lb)	Ideal jet thrust $F_{J,i}$ (lb)	Actual jet thrust $F_{J,a}$ (lb)	Air flow $W_{a,1}$ (lb/sec)	Fuel flow W_f (lb/hr)	Specific fuel consumption $W_f/W_{n,a}$ (lb/lb hr) (lb thrust)	Exhaust- gas tempera- ture T_g (°R)	Engine total pressure ratio P_g/P_2	Engine total- temperature ratio T_g/T_2
1	15,000	1.505	0.625	1183	0.757	464	500	7280	415	4768	4546	6947	6528	106.21	5555	1.978	1532	1.955	3.064
		1.291	.618	1188	.745	461	498	7280	442	4358	3856	6506	6108	106.61	4885	1.250	1425	1.622	2.875
		1.292	.618	1183	.752	465	500	7280	455	4014	3642	6151	5779	105.51	4615	1.287	1346	1.747	2.752
		1.294	.621	1183	.754	465	501	7280	511	3359	2847	5808	5087	105.50	3605	1.528	1257	1.676	2.469
		1.294	.628	1183	.759	472	508	6718	528	2994	1837	4272	3812	95.99	2905	1.576	1122	1.396	2.209
		1.295	.616	1188	.759	475	509	5854	535	1982	1607	5875	5803	92.88	1077	1.621	1077	1.398	2.116
		1.295	.625	1188	.749	469	508	5806	538	—	586	—	2456	77.64	1680	2.045	941	1.063	1.853
		1.291	.616	1190	.751	477	513	5082	535	218	187	1471	1422	81.25	1180	0.946	874	.948	1.704
		1.284	.609	1190	.739	472	507	5695	535	-195	-254	700	640	44.30	775	—	780	.668	1.556
		1.287	.612	1184	.741	466	505	5086	538	-530	-534	529	523	38.70	584	—	682	.812	1.556
11	35,000	0.017	0.185	477	0.276	445	445	7280	435	2044	1886	2825	2087	58.48	2070	1.098	1585	2.110	3.617
		1.020	.189	478	.278	441	444	7280	435	2040	1889	2829	2088	58.84	2071	1.096	1586	2.101	3.608
		1.014	.341	478	.278	442	444	7280	475	1610	1611	1875	1644	38.46	1760	1.141	1406	1.818	3.171
		1.018	.363	478	.261	441	443	7280	535	1580	1588	1749	1584	38.78	1810	1.096	1481	1.754	2.847
		1.013	.264	478	.260	440	442	7078	535	1494	1548	1863	1529	38.57	1486	1.060	1217	1.705	2.763
		1.019	.364	478	.267	437	438	6718	535	1547	1581	1853	1537	38.50	1508	1.151	1385	1.654	2.625
		1.081	.278	478	.269	458	458	6006	535	800	707	960	887	29.08	935	1.332	1084	1.562	2.333
		1.022	.178	478	.264	457	440	5083	535	108	170	260	281	14.34	740	1.618	1011	1.212	2.296
		1.022	.176	478	.256	457	440	5963	535	110	124	169	194	12.87	726	4.333	1065	1.065	2.459
		1.023	.173	478	.266	457	440	5830	535	91	100	155	162	10.33	683	6.850	1130	1.053	2.568
24	40,000	1.290	.814	477	.350	410	448	7280	426	2371	2106	3165	2063	46.78	2615	1.208	1645	2.158	5.491
		1.299	.835	478	.301	411	445	7280	426	2084	1818	3165	2059	46.75	2115	1.211	1840	2.158	5.478
		1.303	.839	478	.300	410	442	7280	427	2012	1881	2935	2012	47.48	2220	1.174	1400	1.946	3.187
		1.301	.825	478	.300	410	442	7280	465	1979	1797	2894	1741	47.45	2220	1.174	1756	1.934	3.118
		1.292	.816	482	.300	410	441	7280	510	1874	1838	2677	1441	47.81	1805	1.258	1862	1.742	2.862
		1.299	.863	479	.350	411	445	7078	535	1481	1536	2358	1912	47.10	1713	1.265	1177	1.695	2.857
		1.297	.861	478	.350	411	445	6718	535	1481	1587	2112	1812	48.58	1615	1.338	1105	1.564	2.490
		1.281	.816	480	.350	410	441	5854	535	1145	1080	1928	1487	44.80	1882	1.321	1202	1.812	2.458
		1.282	.858	476	.360	409	441	5086	535	—	533	—	1877	38.00	934	1.780	882	1.205	2.176
		1.298	.863	476	.360	410	441	5086	535	—	531	—	785	29.98	702	4.106	881	1.015	1.852
34	45,000	1.291	.811	477	.350	412	444	5985	535	—	531	—	373	20.14	512	—	747	1.582	3.054
		1.293	.832	477	.350	410	445	5086	535	—	531	—	150	15.81	507	—	697	1.582	3.054
		1.295	.866	478	.350	410	445	7280	444	3024	2925	4556	4554	45.85	1620	2.046	1620	2.046	5.387
		1.296	.864	478	.354	410	445	7280	444	2975	2925	4556	4554	45.85	1620	2.047	1620	2.047	5.387
		1.297	.864	478	.354	410	445	7280	444	2975	2925	4556	4554	45.85	1620	2.048	1620	2.048	5.387
		1.298	.862	478	.354	410	445	7280	444	2975	2925	4556	4554	45.85	1620	2.049	1620	2.049	5.387
		1.299	.862	478	.354	410	445	7280	444	2975	2925	4556	4554	45.85	1620	2.050	1620	2.050	5.387
		1.295	.878	478	.354	410	445	7280	444	2975	2925	4556	4554	45.85	1620	2.051	1620	2.051	5.387
		1.293	.878	478	.354	410	445	7280	444	2975	2925	4556	4554	45.85	1620	2.052	1620	2.052	5.387
		1.294	.878	478	.354	410	445	7280	444	2975	2925	4556	4554	45.85	1620	2.053	1620	2.053	5.387
		1.295	.878	478	.354	410	445	7280	444	2975	2925	4556	4554	45.85	1620	2.054	1620	2.054	5.387
54	60,000	1.291	.819	222	0.168	404	435	7280	442	1592	1274	1835	1818	26.80	1840	1.287	1504	2.125	3.450
		1.288	.811	290	.294	407	435	7280	455	1401	1320	1840	1848	28.72	1848	1.289	1515	2.127	3.442
		1.284	.809	292	.291	408	435	7280	467	1485	1141	1785	1878	26.70	1845	1.345	1582	1.945	3.178
		1.285	.816	289	.210	408	435	7280	480	1485	1047	1723	1878	26.68	1845	1.345	1582	1.945	3.178
		1.284	.819	289	.210	408	435	7280	535	1057	870	1643	1878	26.61	1845	1.345	1582	1.945	3.178
		1.287	.807	291	.211	412	442	7078	535	585	594	820	1280	26.54	1243	1.581	1215	1.788	2.761
		1.285	.808	291	.212	411	441	7118	535	585	594	820	1280	26.47	1243	1.581	1215	1.788	2.761
		1.290	.821	218	.215	408	434	6534	535	820	815	1246	1246	32.43	1000	1.370	1133	1.692	2.869
		1.289	.806	281	.211	411	441	5808	535	400	513	751	821	24.45	926	1.404	1022	1.511	2.882
		1.292	.806	285	.214	411	441	5808	535	250	185	547	480	15.11	689	3.801	1027	1.189	2.122
64	65,000	1.294	0.619	222	0.168	404	435	7280	442	1087	1002	1809	1424	22.88	1292	1.288	1632	2.098	3.492
		1.303	.823	223	.168	405	435	7280	447	1087	1024	1845	1424	22.93	1292	1.289	1632	2.098	3.492
		1.298	.823	223	.168	405	435	7280	471	1087	1024	1845	1424	22.78	1292	1.287	1632	2.096	3.492
		1.299	.824	223	.167	405	435	7280	485	985	980	1275	1424	22.85	1292	1.287	1632	2.097	3.492
		1.294	.809	224	.168	405	435	7280	535	820	815	1246	1246	22.88	1292	1.288	1632	2.098	3.492
		1.292	.826	183	.122	411	445	7280	537	820	815	1246	1246	2					

2733

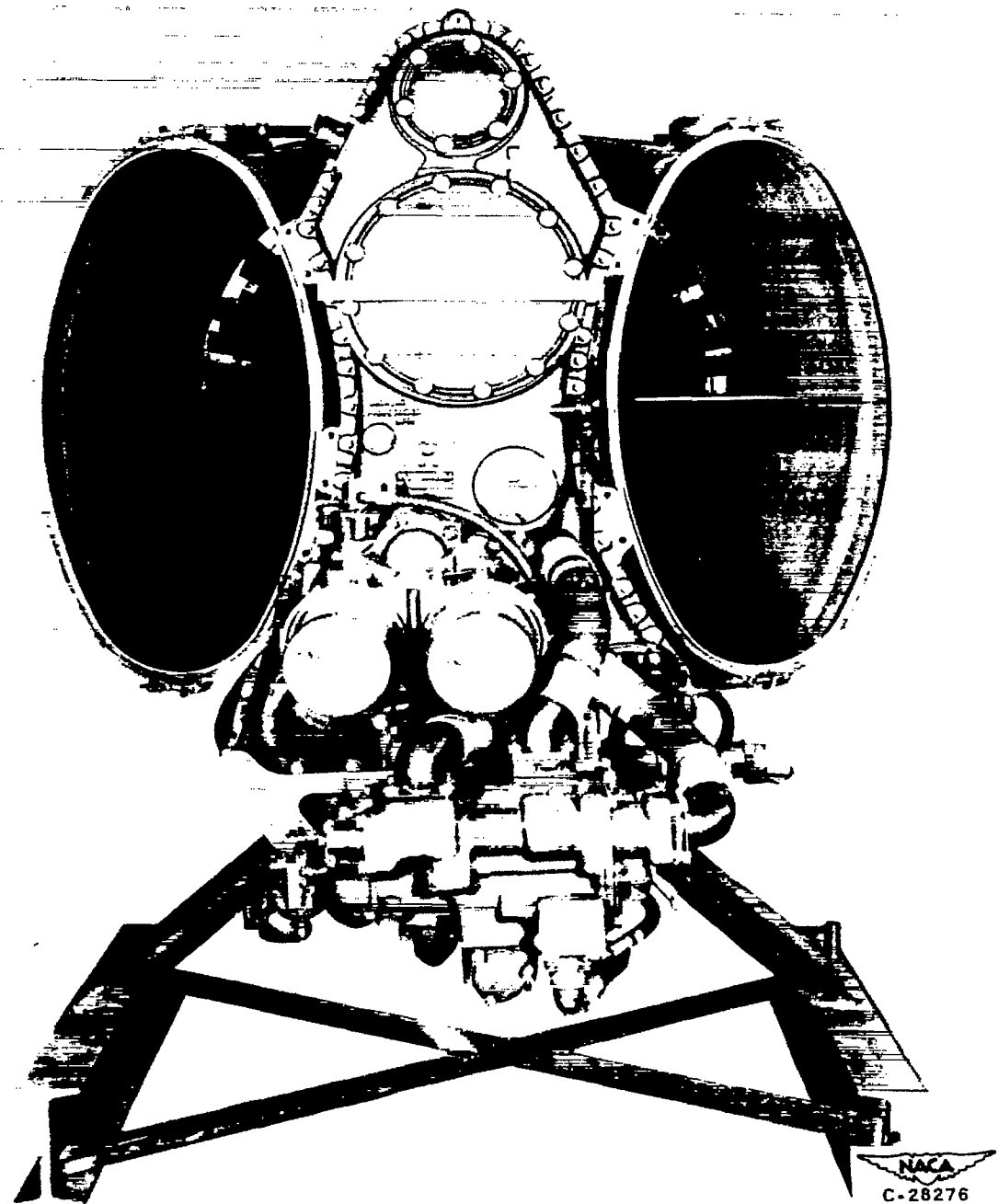


Figure 1. - View looking downstream of inlet of prototype J40-WE-8 turbojet engine.

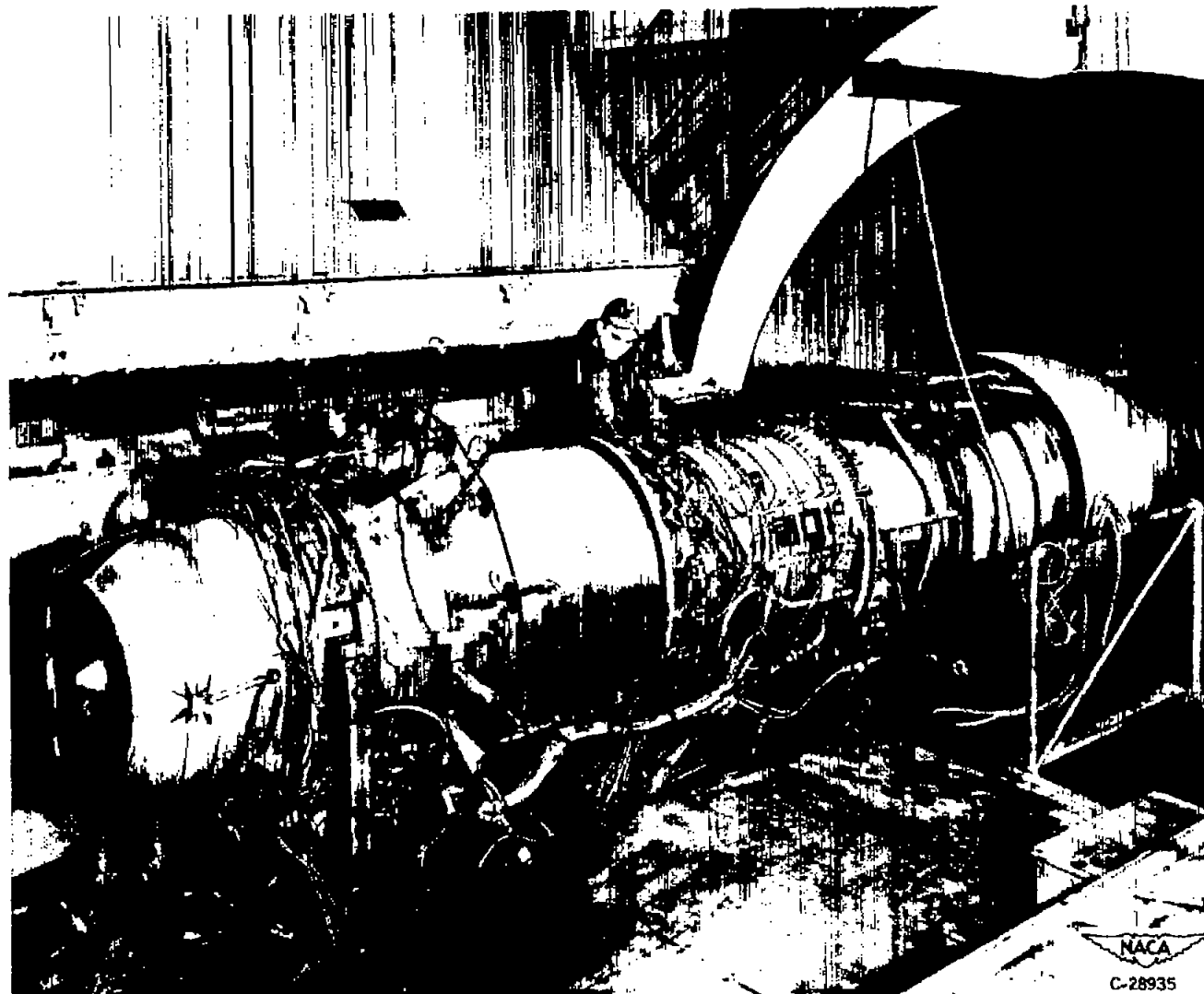
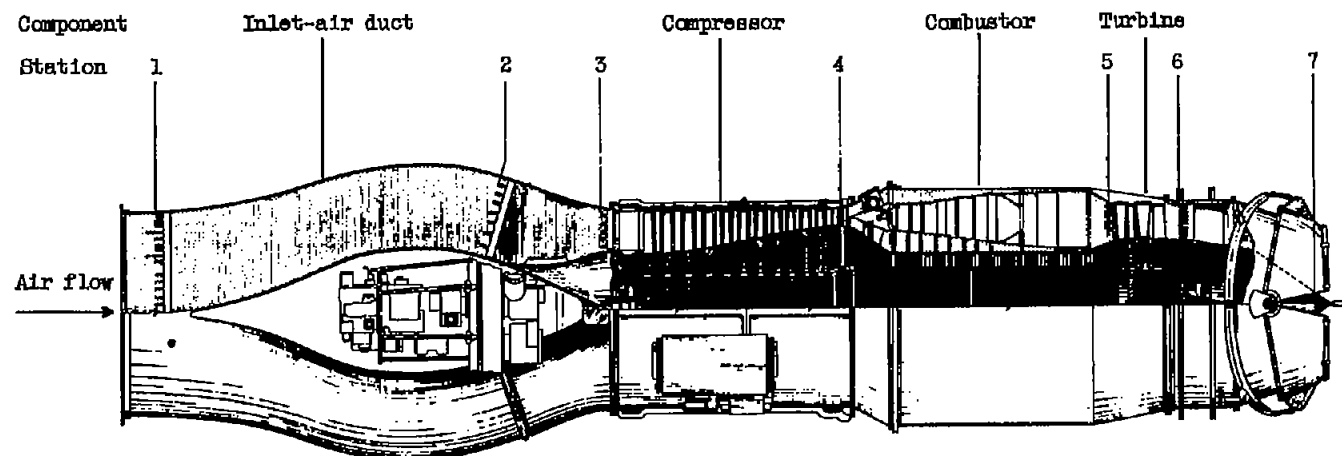


Figure 2. - Prototype J40-WE-8 turbojet engine installed in test section of altitude wind tunnel.

NACA RM E52K10



Station	Location	Total-pressure tubes	Static-pressure tubes	Wall static-pressure orifices	Thermocouples
1	Inlet-air duct	29	12	6	10
2	Engine inlet	18	0	4	0
3	Compressor inlet	23	5	7	0
4	Compressor outlet	18	0	3	6
5	Turbine inlet	5	0	0	10 ^a
6	Turbine outlet	20	0	8	24
7	Exhaust-nozzle inlet	16	2	8	0

^a Sonic flow probes

NACA
CD-2732

Figure 3. - Top view of prototype J40-WE-8 turbojet-engine installation showing stations at which instrumentation was installed.

2733

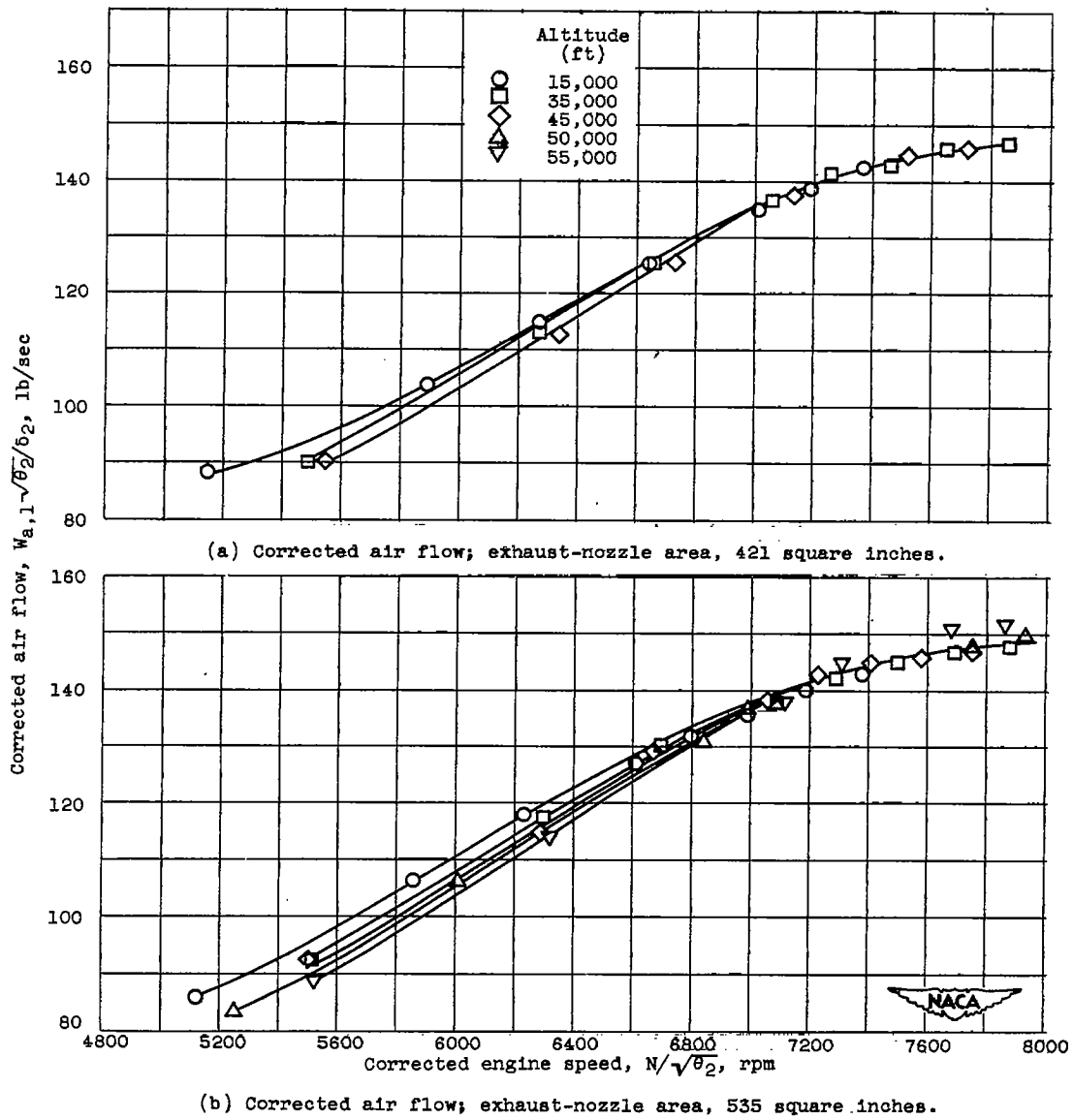


Figure 4. - Effect of altitude on corrected engine performance at flight Mach number of 0.62.

2733

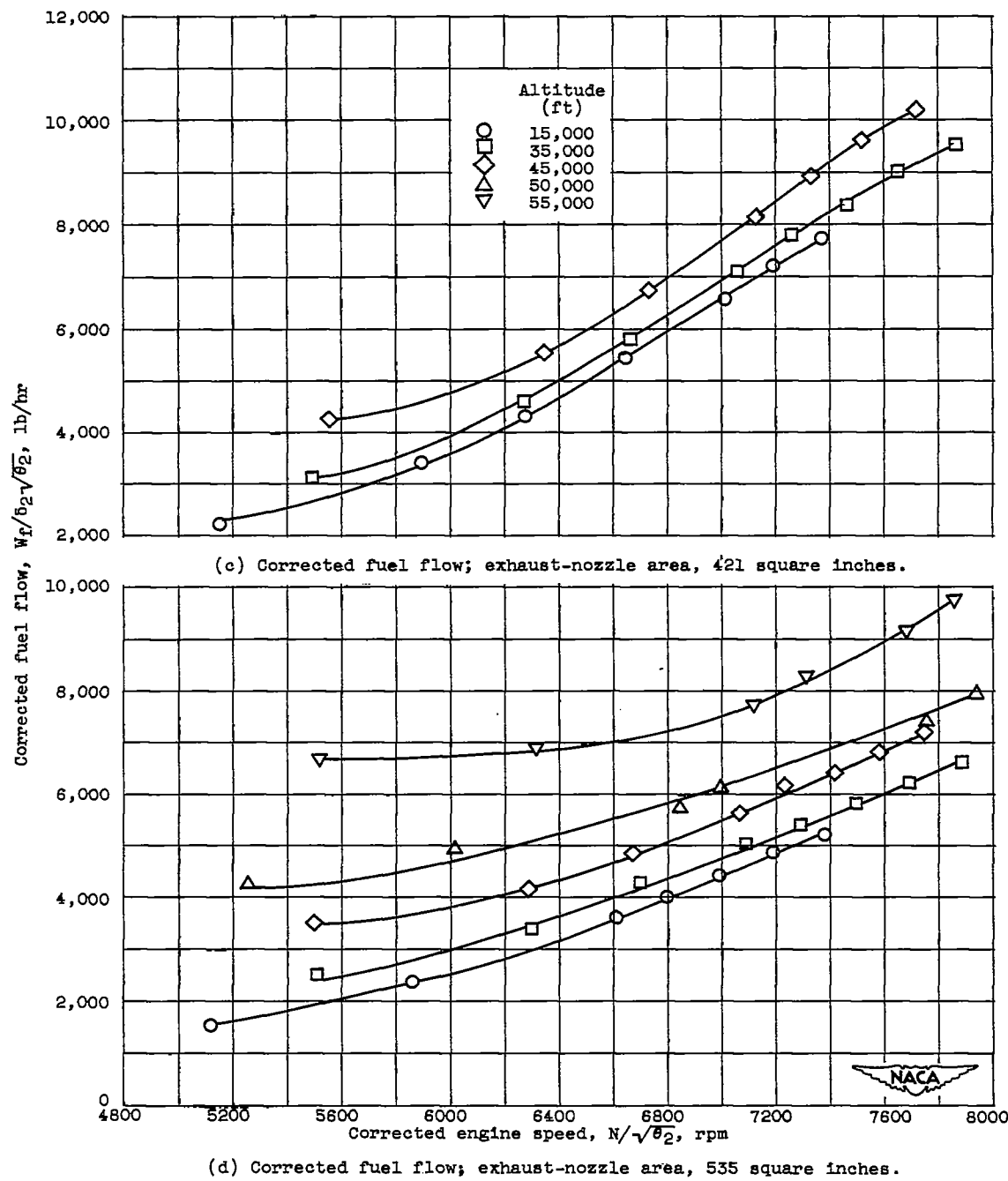


Figure 4. - Continued. Effect of altitude on corrected engine performance at flight Mach number of 0.62.

2733

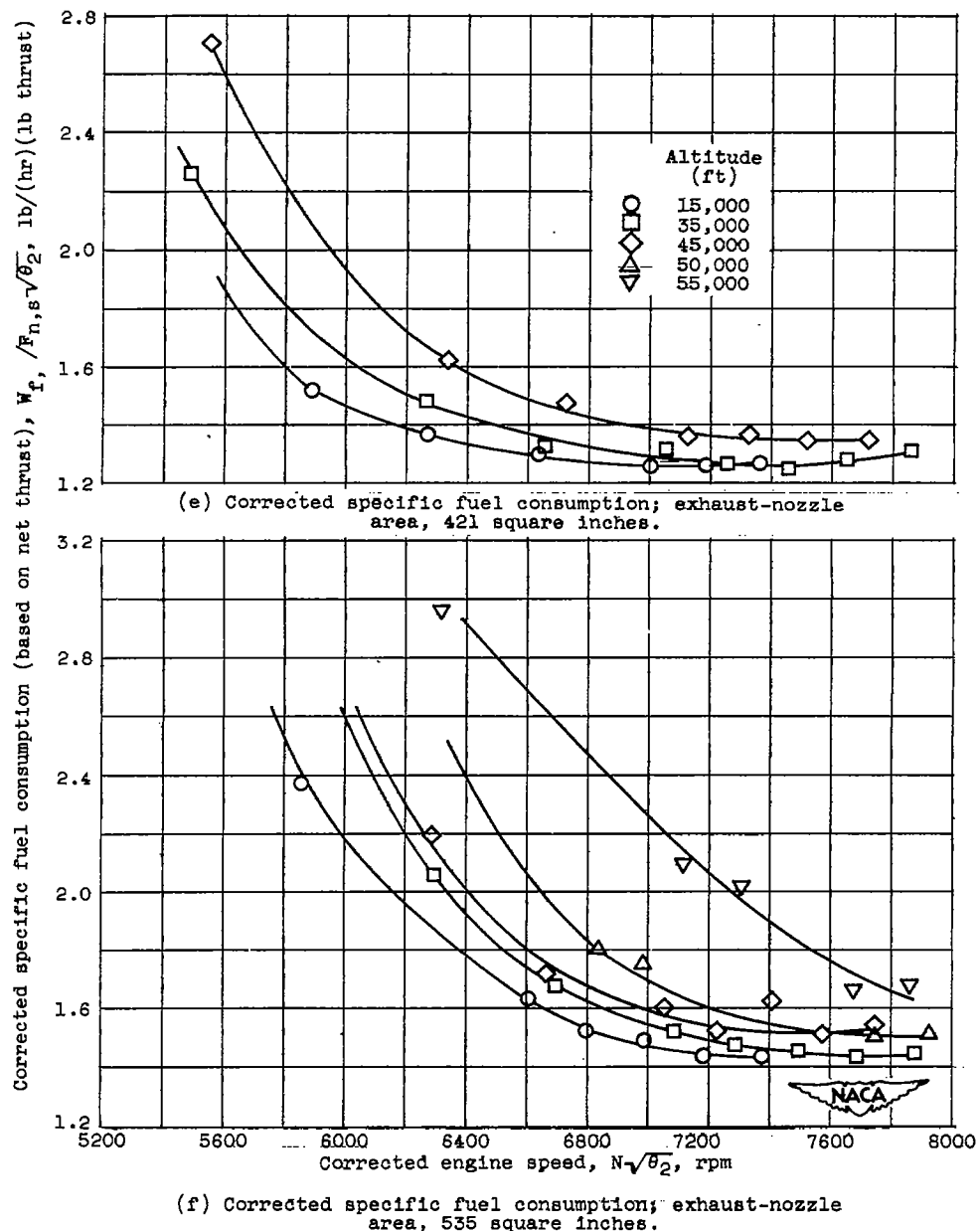
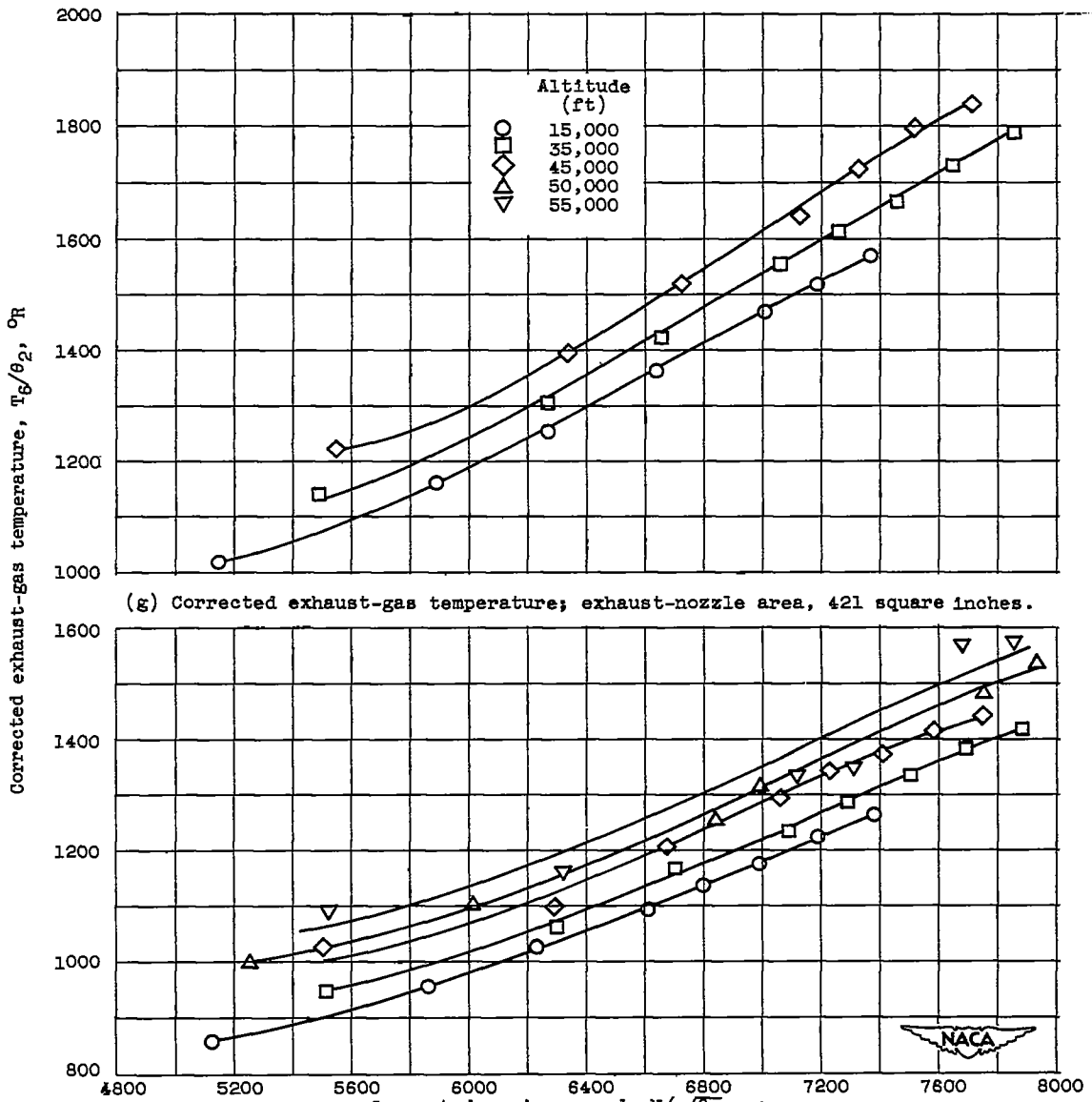


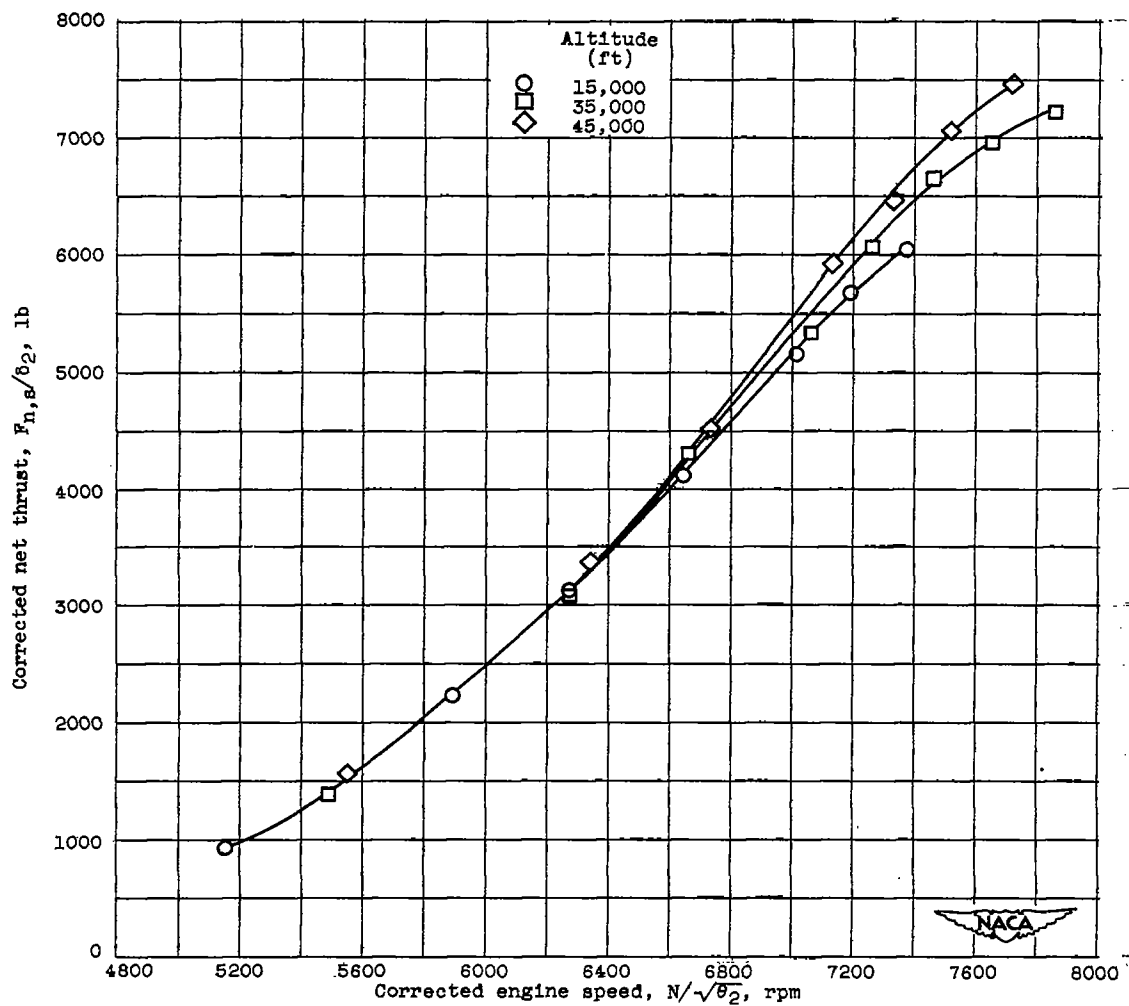
Figure 4. - Continued. Effect of altitude on corrected engine performance at flight Mach number of 0.62.

2733



(h) Corrected exhaust-gas temperature; exhaust-nozzle area, 535 square inches.

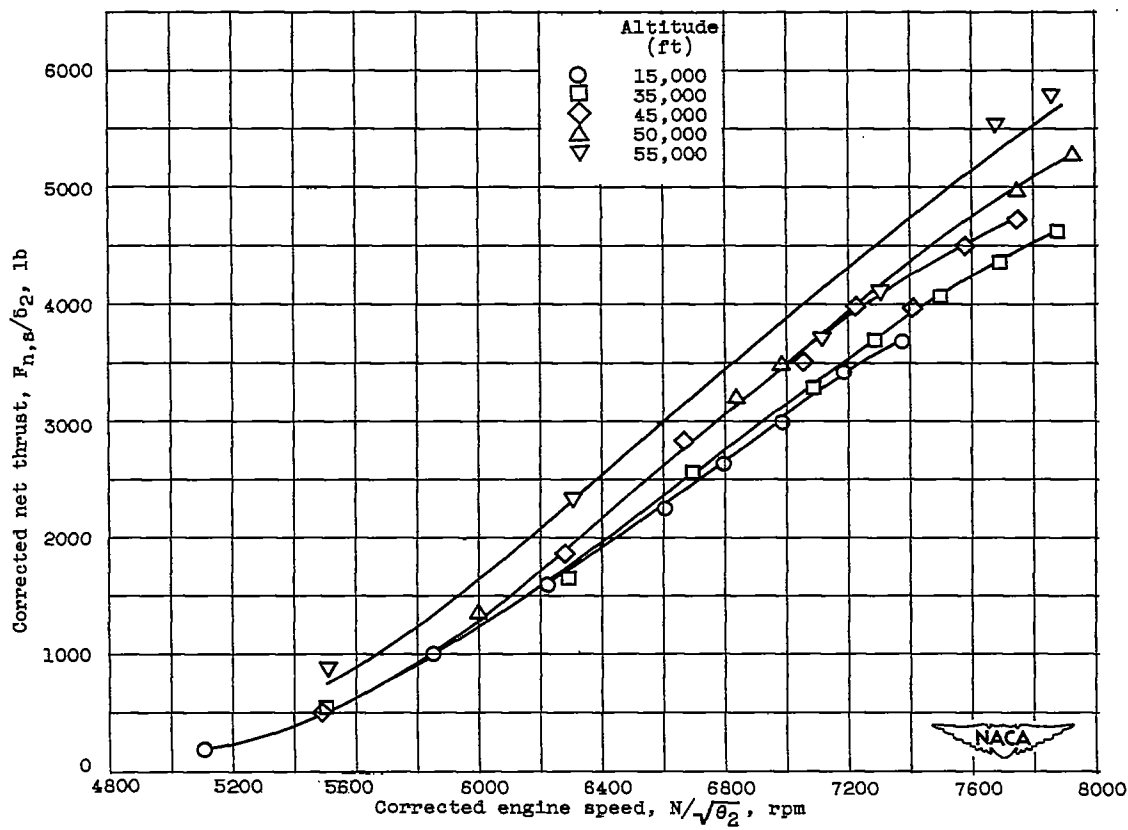
Figure 4. - Continued. Effect of altitude on corrected engine performance at flight Mach number of 0.62.



(i) Corrected net thrust; exhaust-nozzle area, 421 square inches.

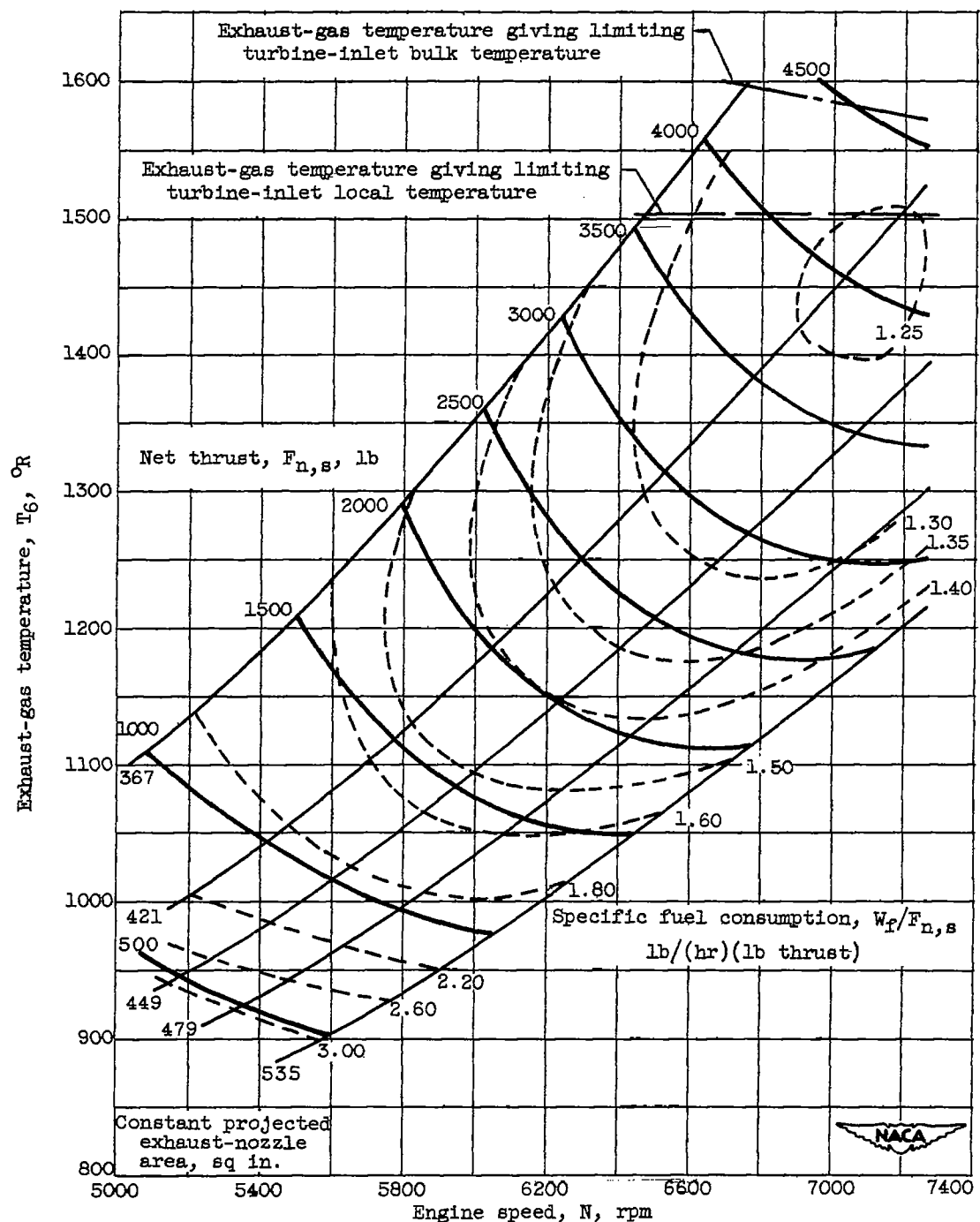
Figure 4. - Continued. Effect of altitude on corrected engine performance at a flight Mach number of 0.62.

2733



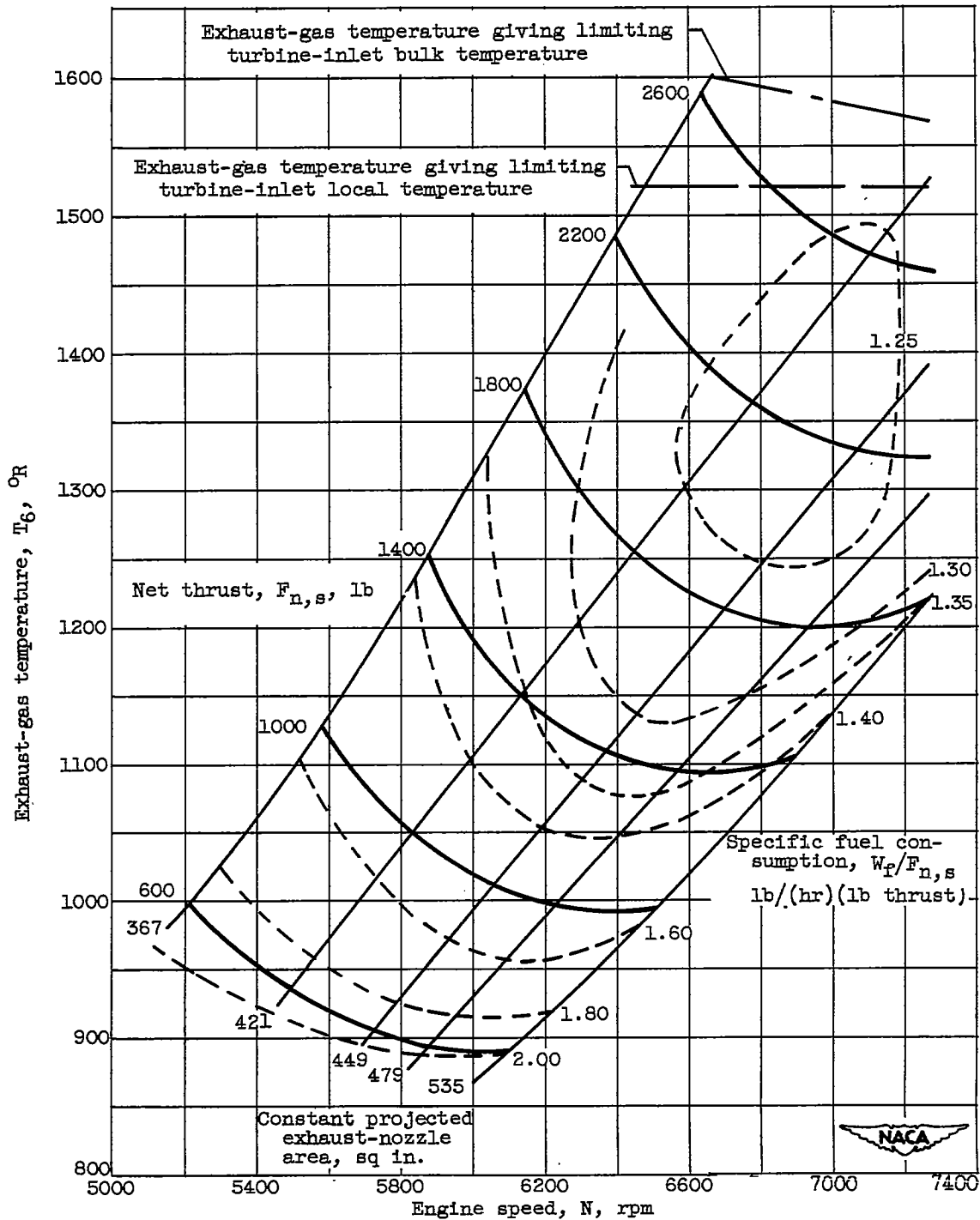
(j) Corrected net thrust; exhaust-nozzle area, 535 square inches.

Figure 4. - Concluded. Effect of altitude on corrected engine performance at a flight Mach number of 0.62.



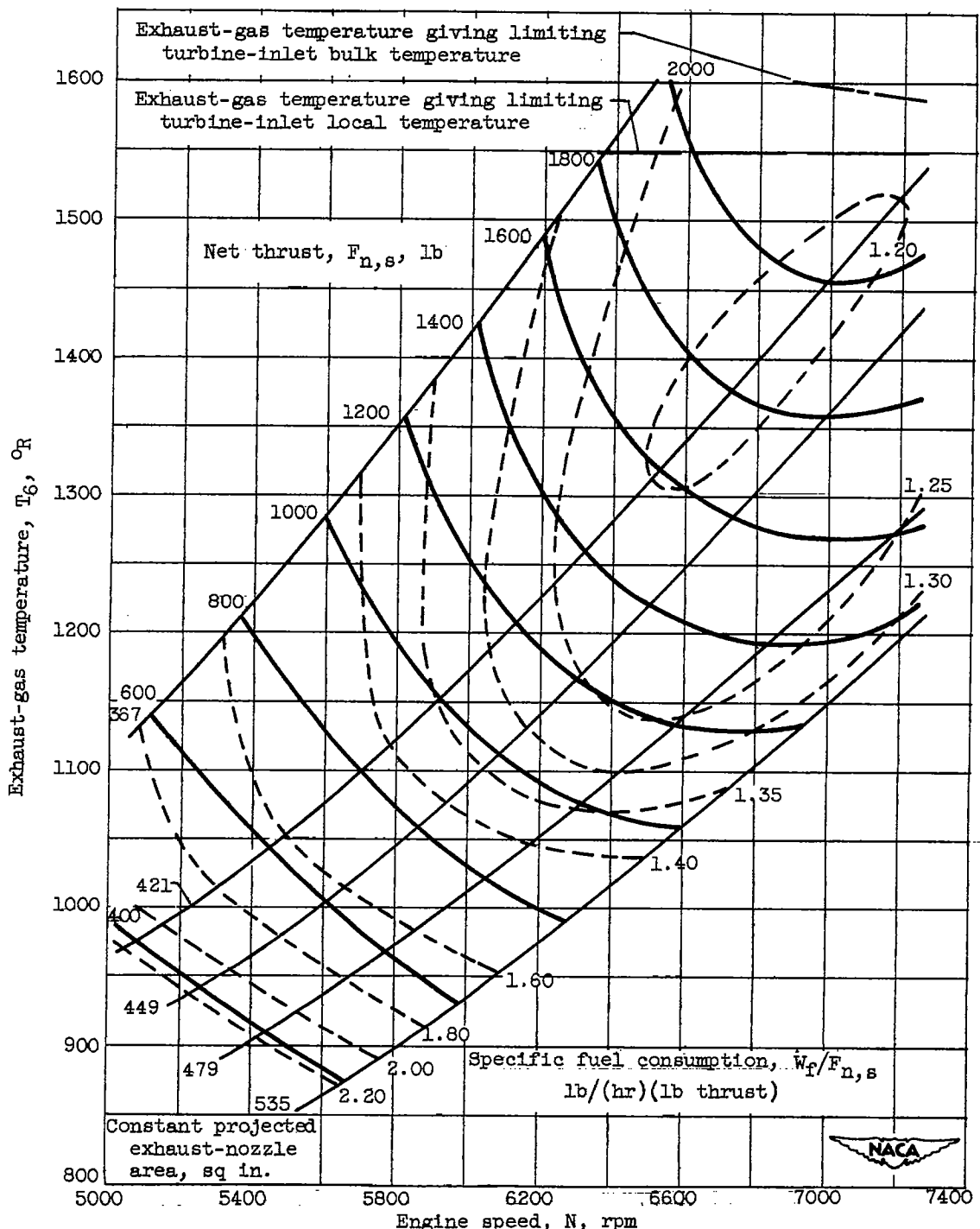
(a) Altitude, 15,000 feet; flight Mach number, 0.62; equivalent inlet-air temperature, 468° R.

Figure 5. - Engine performance maps.



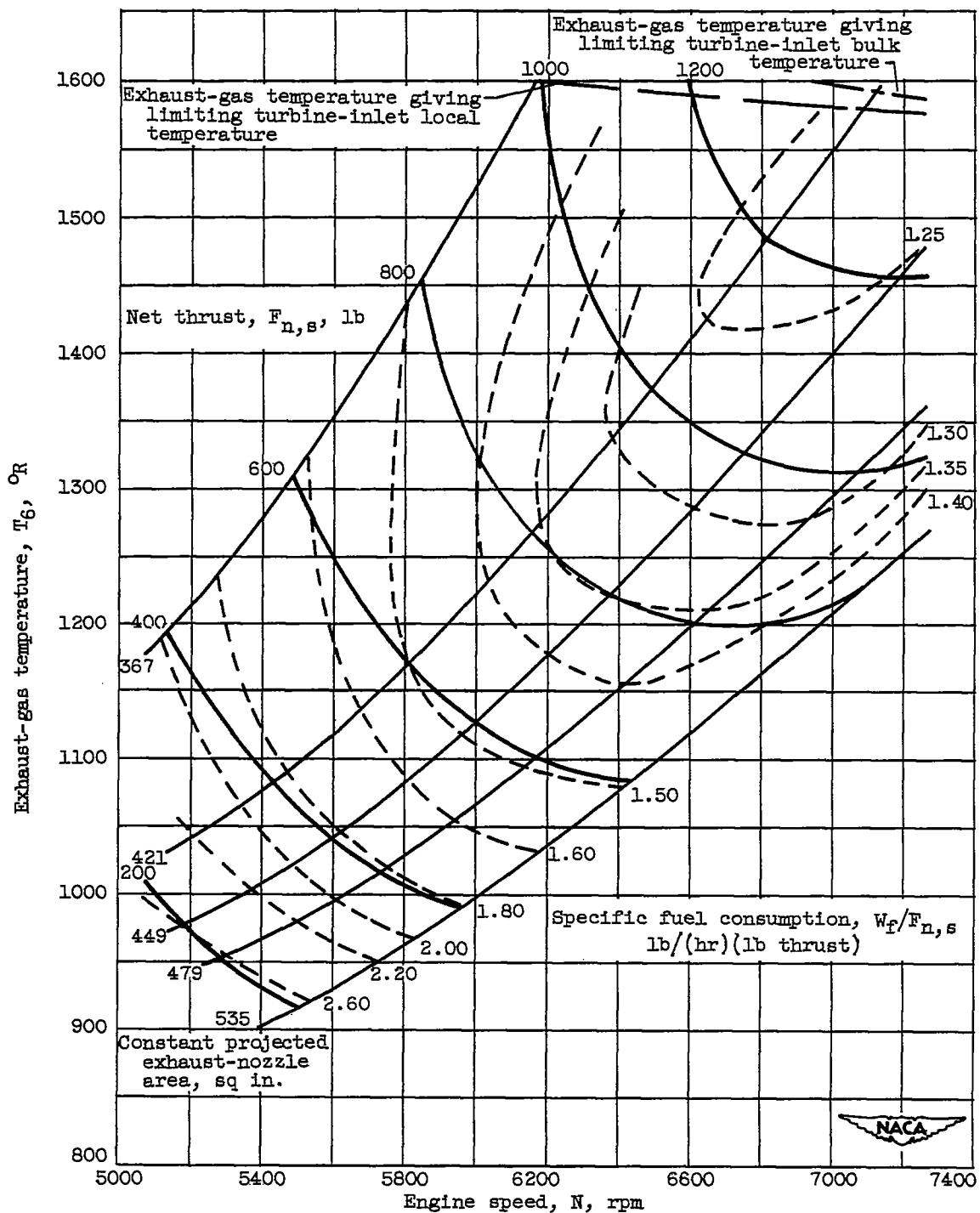
(b) Altitude, 35,000 feet; flight Mach number, 0.99; equivalent inlet-air temperature, 393° R.

Figure 5. - Continued. Engine performance maps.



(c) Altitude, 35,000 feet; flight Mach number, 0.62; equivalent inlet air temperature, 414° R.

Figure 5. - Continued. Engine performance maps.



(d) Altitude, 45,000 feet; flight Mach number, 0.62; equivalent inlet-air temperature, 410° R.

Figure 5. - Concluded. Engine performance maps.

2733

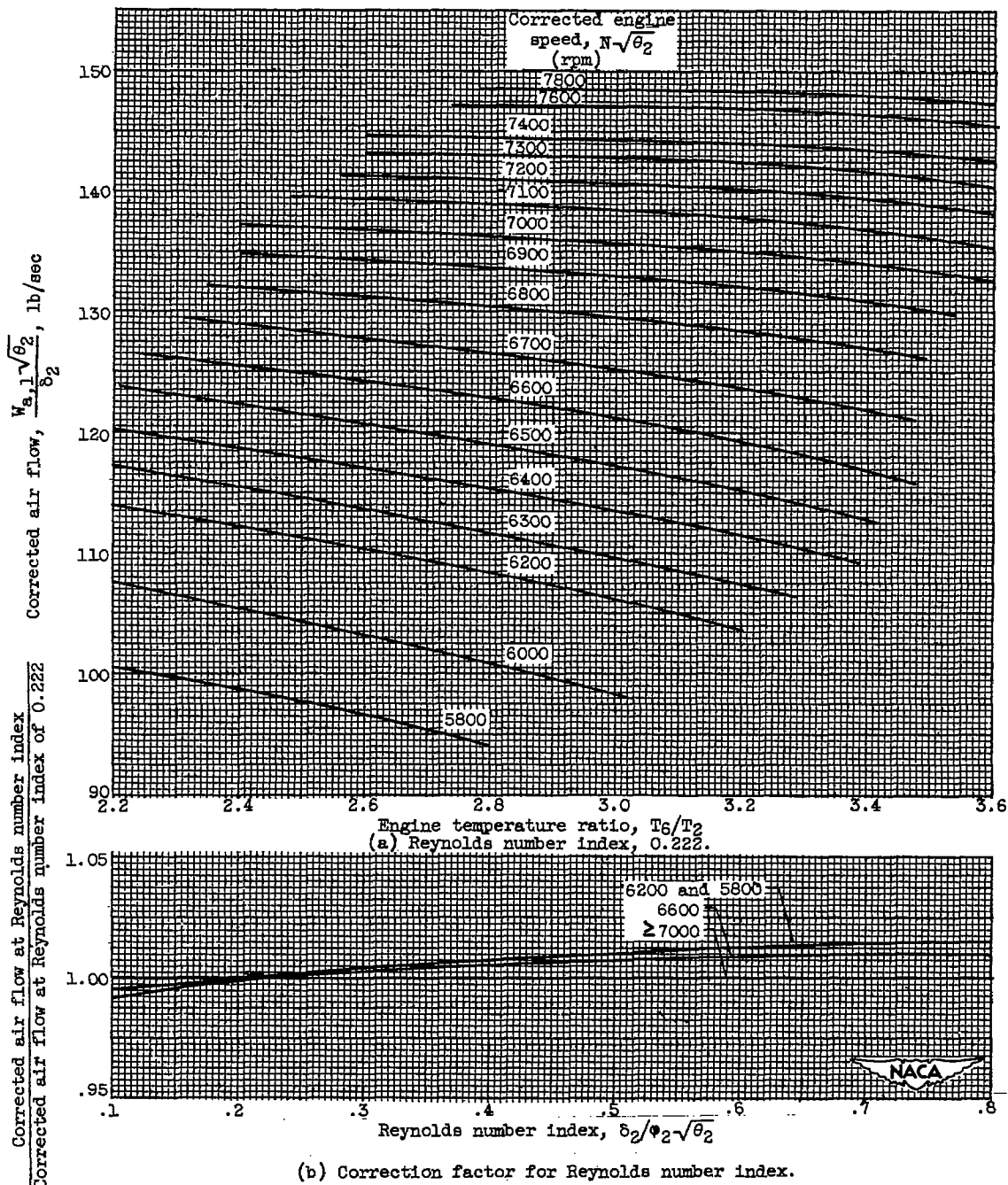


Figure 6. - Variation of corrected air flow with Reynolds number index, corrected engine speed, and engine temperature ratio.

2733

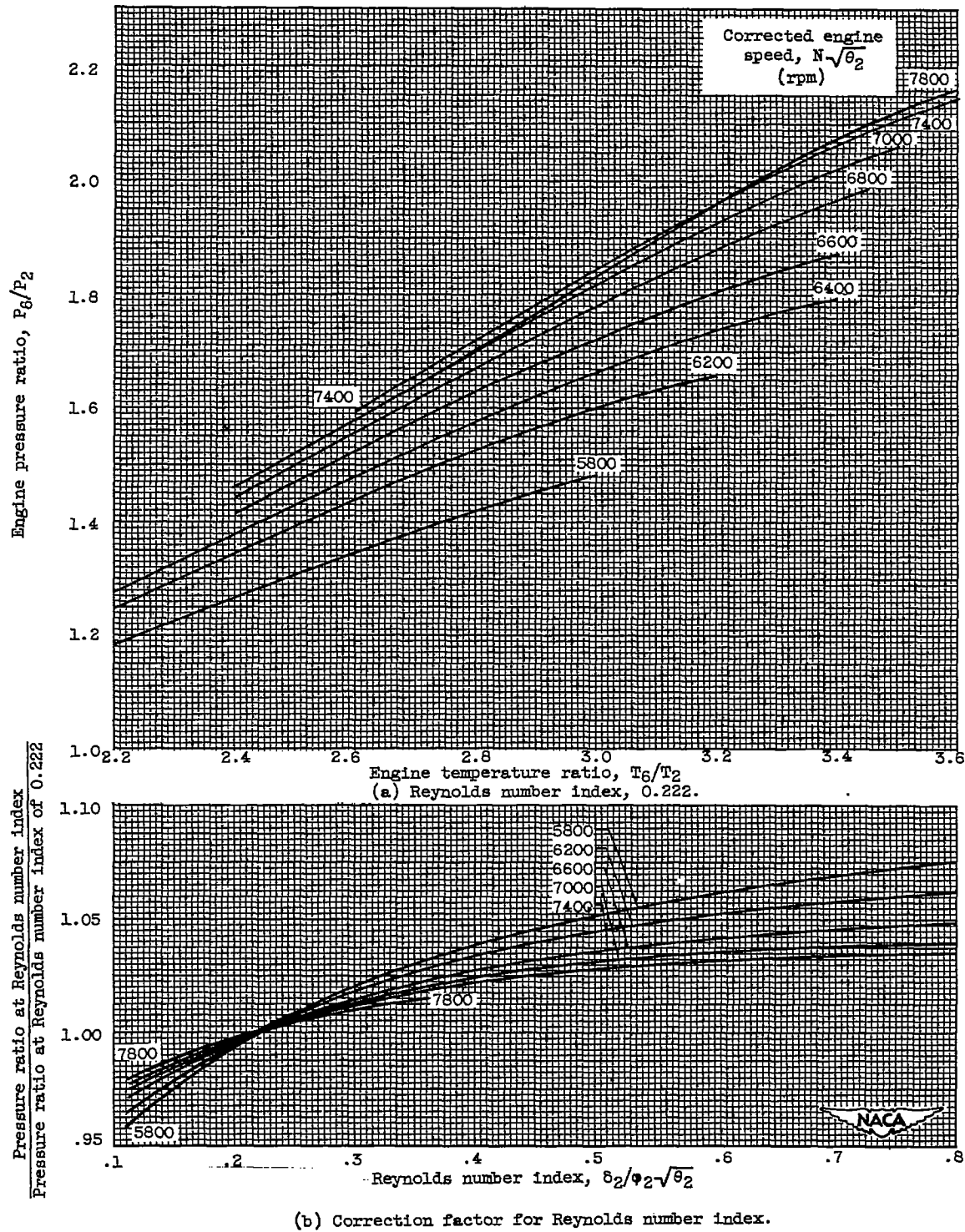


Figure 7. - Variation of engine pressure ratio with Reynolds number index, corrected engine speed, and engine temperature ratio.

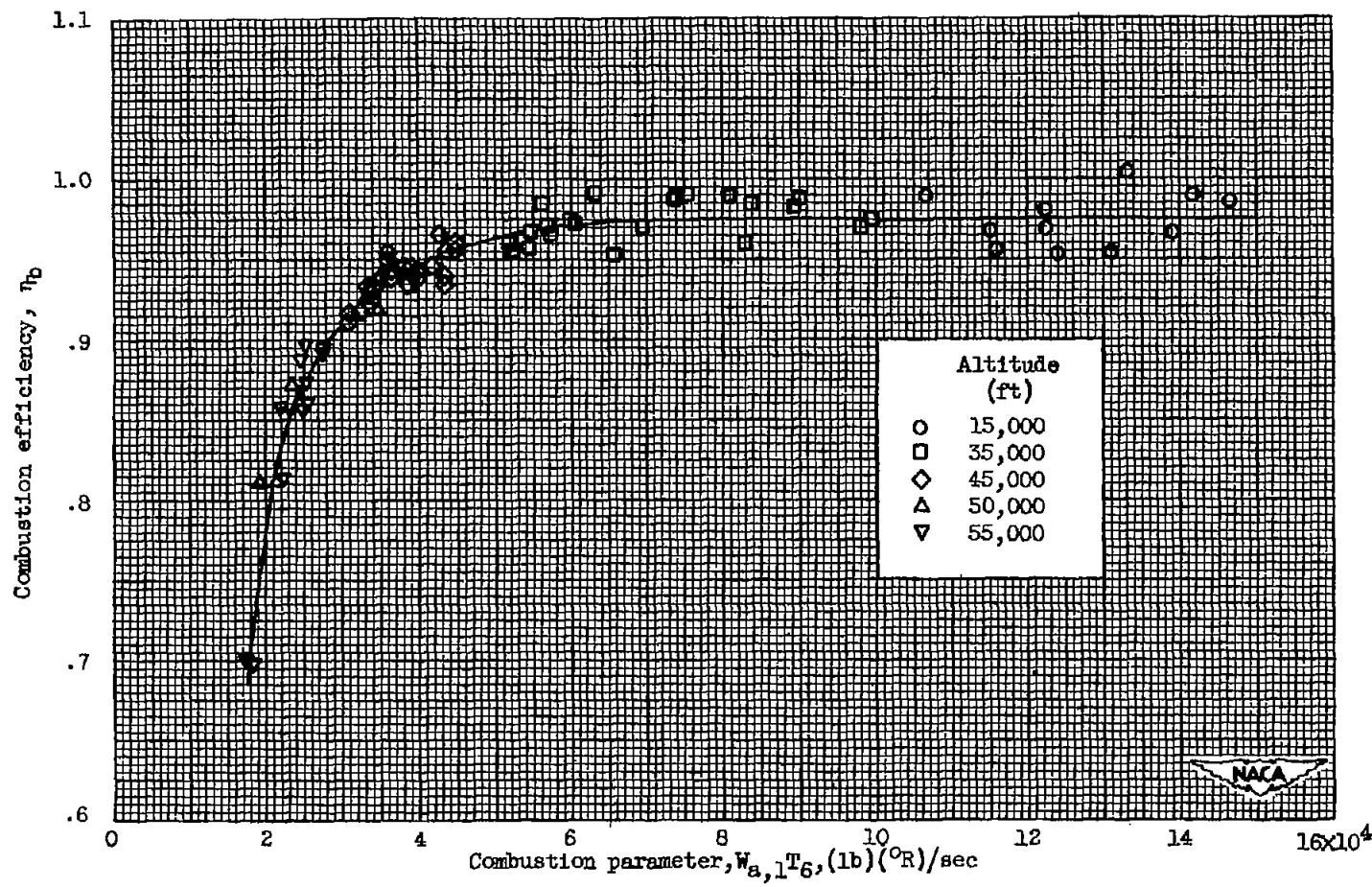


Figure 8. - Variation of combustion efficiency with combustion parameter.

2733

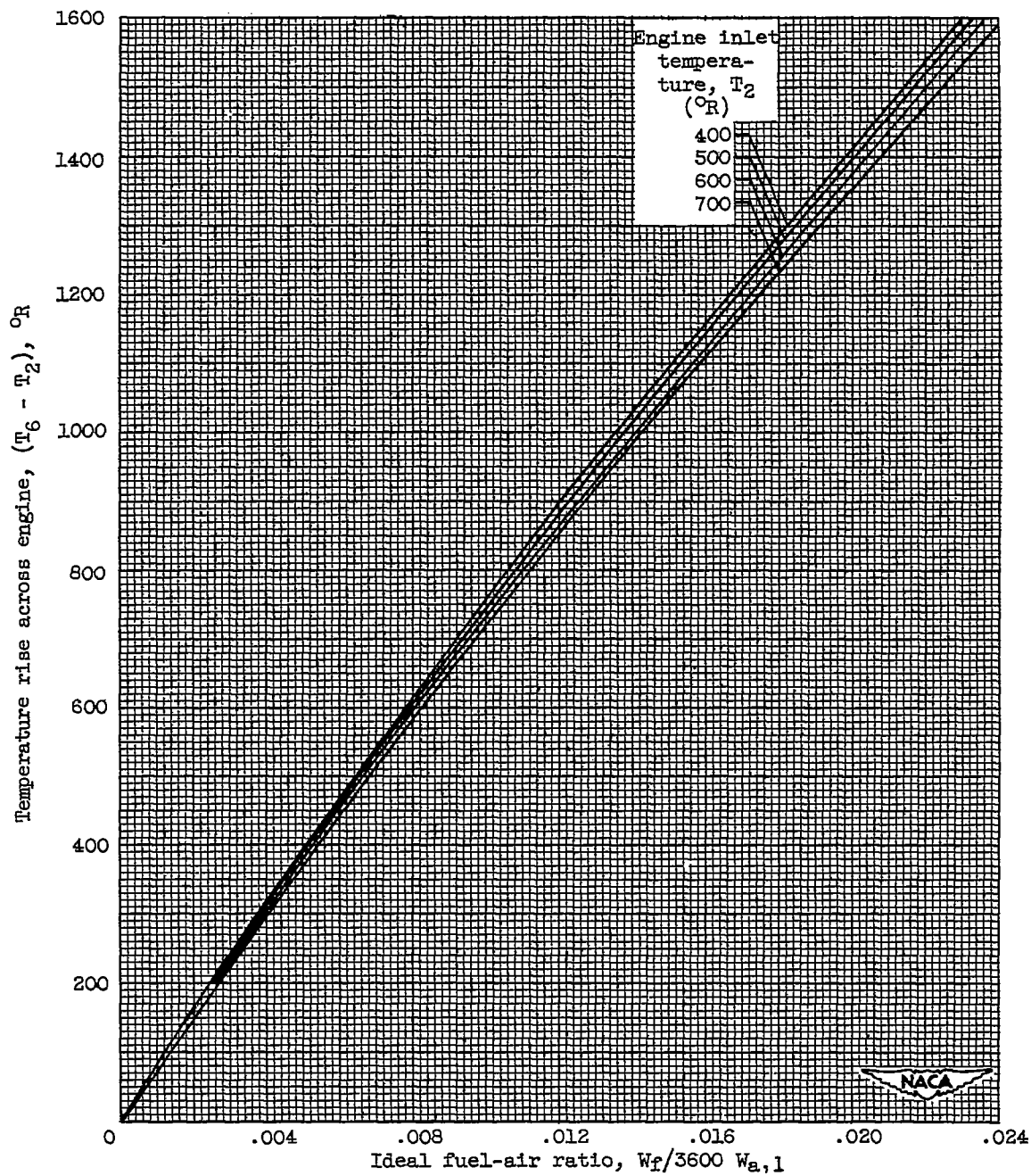


Figure 9. - Engine temperature rise as function of fuel-air ratio. Lower heating value, 18,700 Btu per pound; hydrogen-carbon ratio, 0.171.

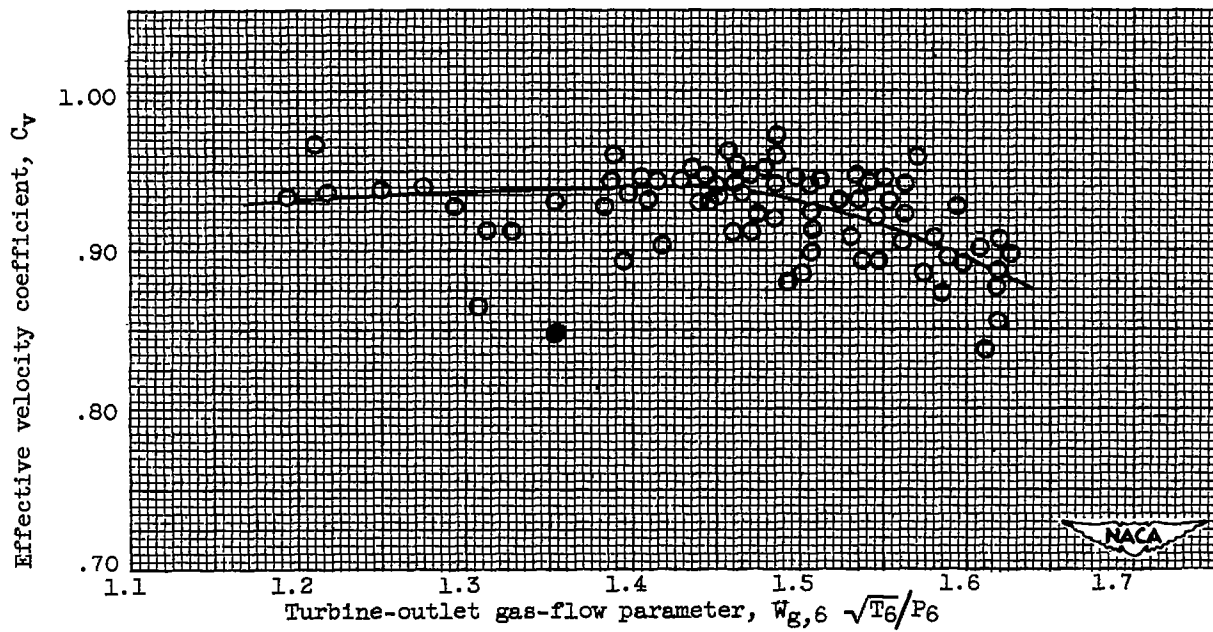
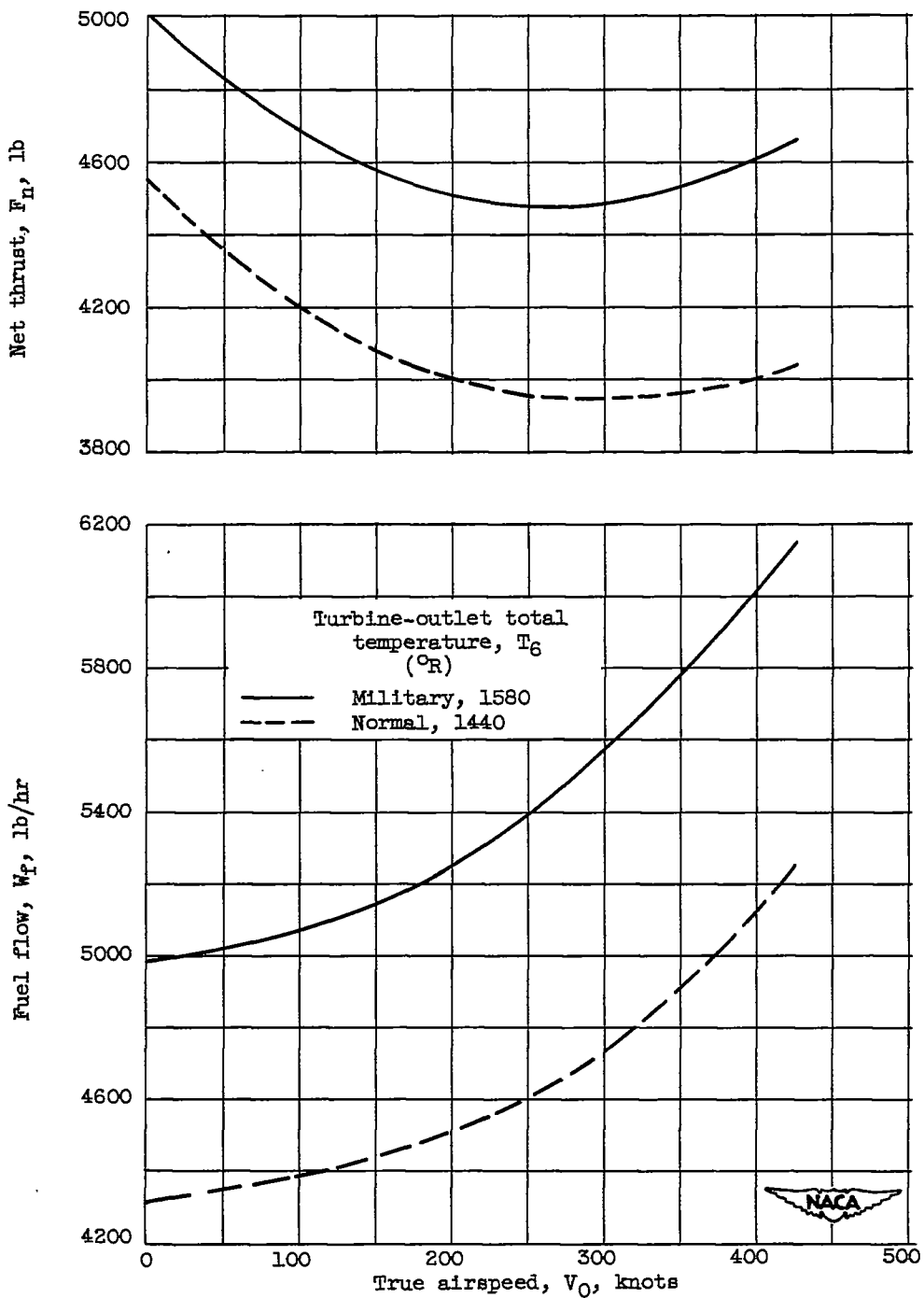


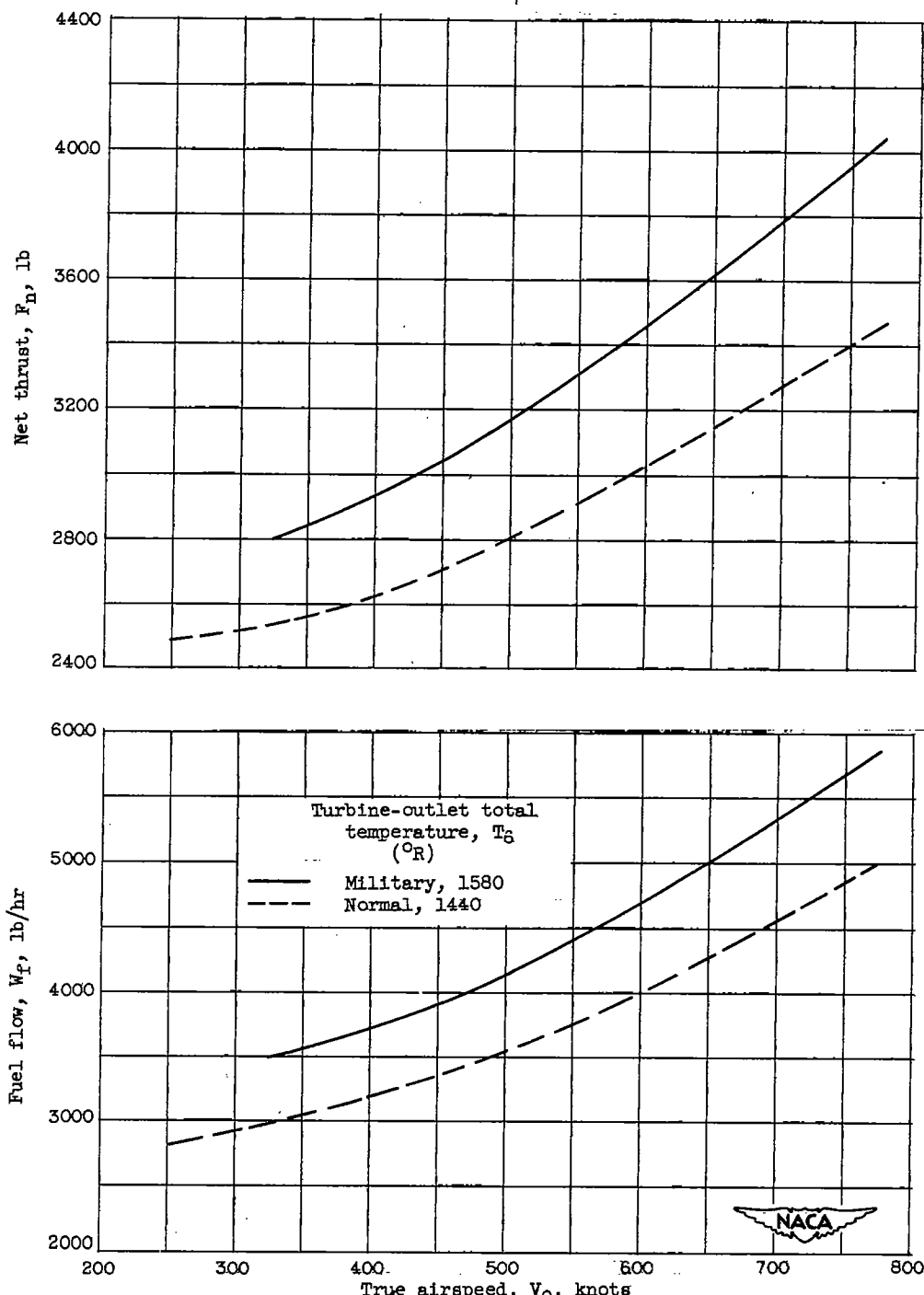
Figure 10. - Variation of effective velocity coefficient with turbine-outlet gas-flow parameter.



(a) Altitude, 15,000 feet.

Figure 11. - Variation of net thrust and fuel flow with flight speed obtained by calculation from pumping characteristics. Engine speed, 7260 rpm.

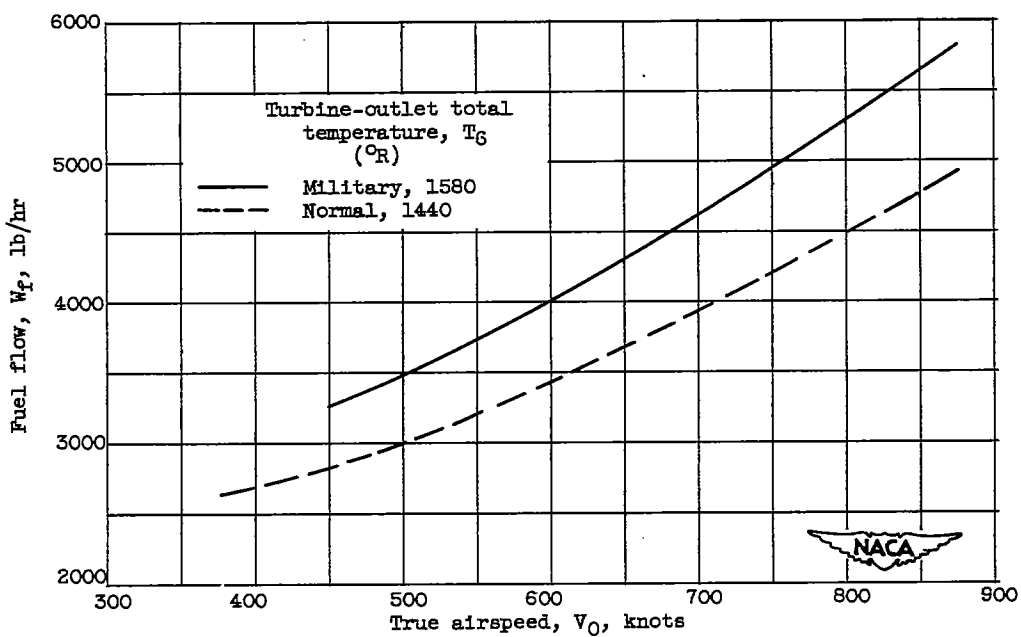
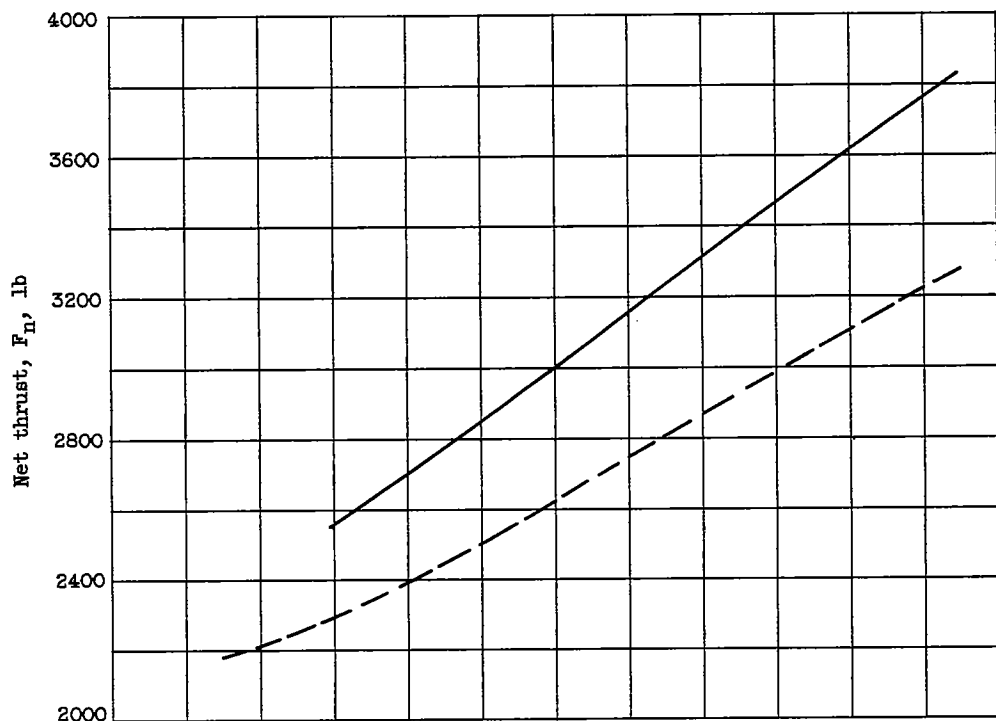
2733



(b) Altitude, 30,000 feet.

Figure 11. - Continued. Variation of net thrust and fuel flow with flight speed obtained by calculation from pumping characteristics. Engine speed, 7260 rpm.

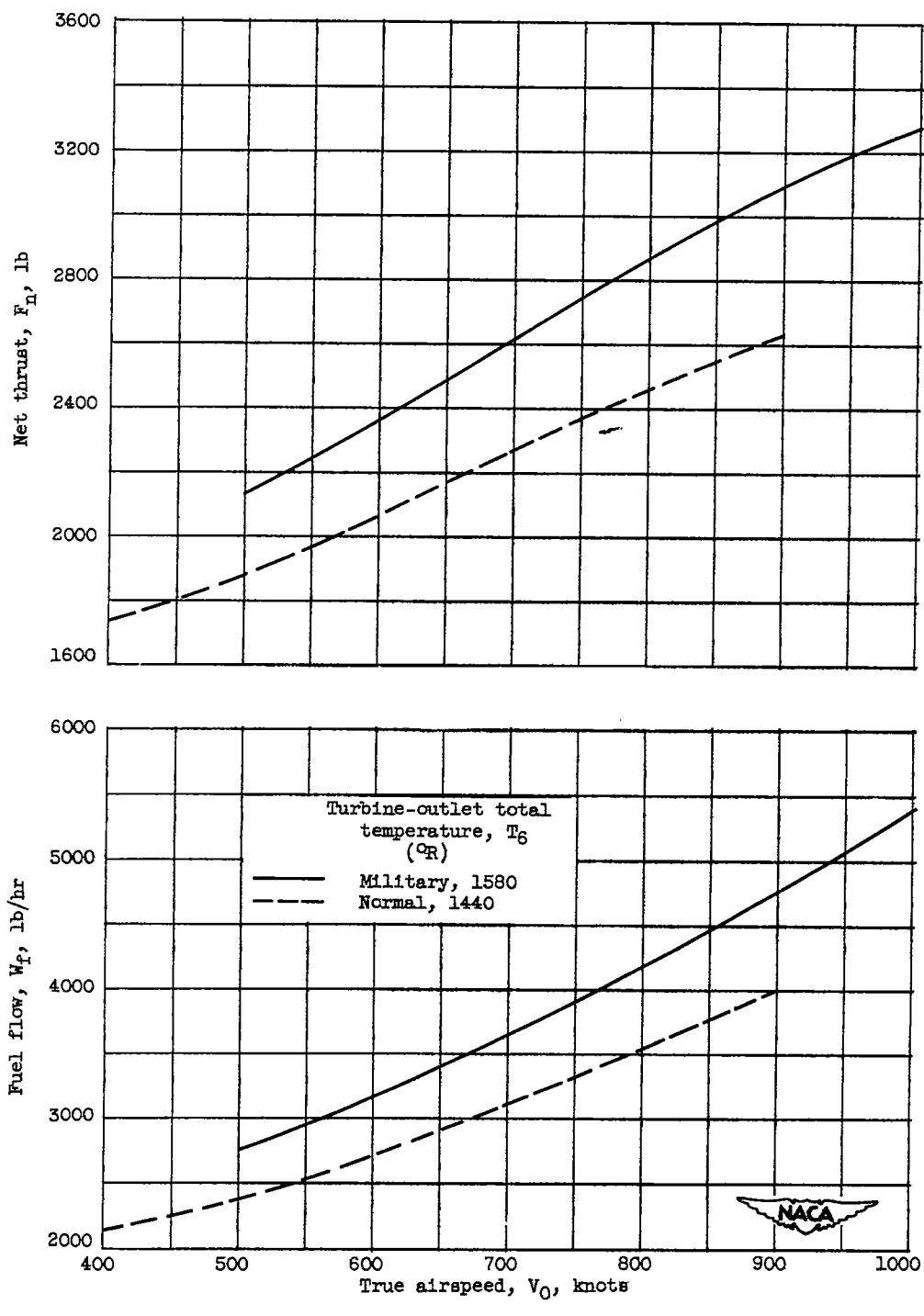
2733



(c) Altitude, 35,000 feet.

Figure 11. - Continued. Variation of net thrust and fuel flow with flight speed obtained by calculation from pumping characteristics. Engine speed, 7260 rpm.

2733



(d) Altitude, 40,000 feet.

Figure 11. - Continued. Variation of net thrust and fuel flow with flight speed obtained by calculation from pumping characteristics. Engine speed, 7260 rpm.

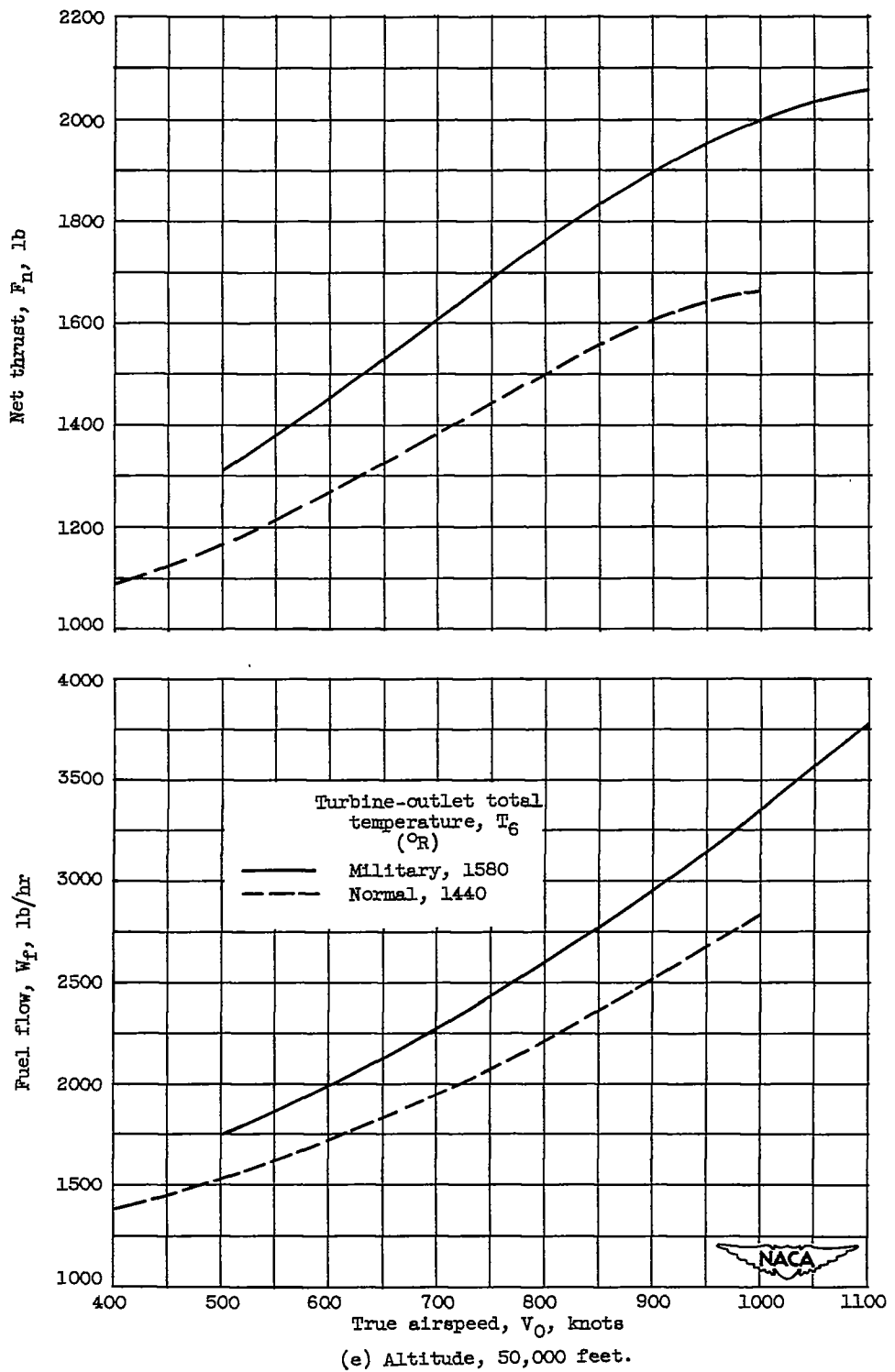


Figure 11. - Concluded. Variation of net thrust and fuel flow with flight speed obtained by calculation from pumping characteristics. Engine speed, 7260 rpm.

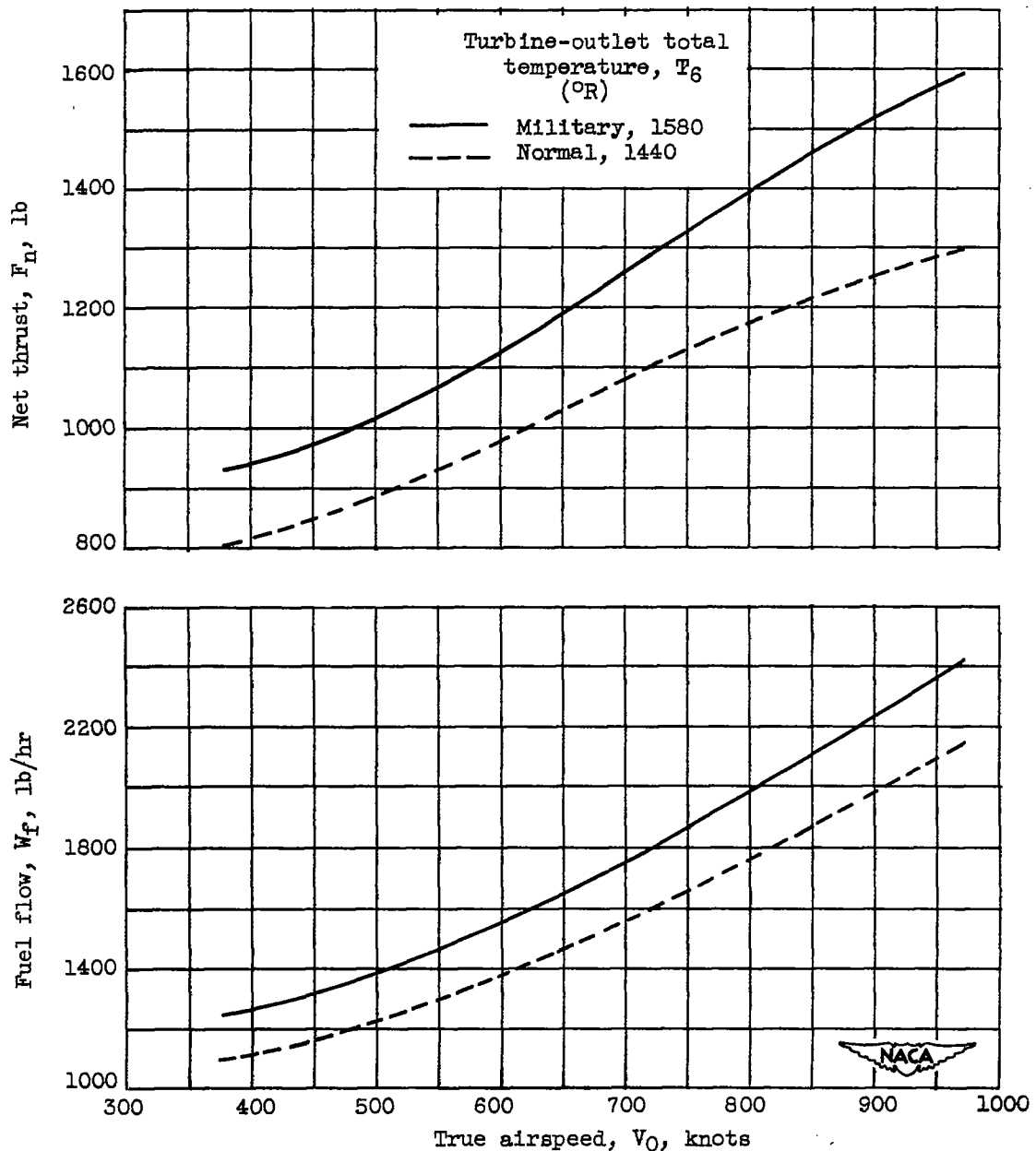


Figure 12. - Variation of net thrust and fuel flow with flight speed from experimental data. Altitude, 55,000 feet; engine speed, 7260 rpm.

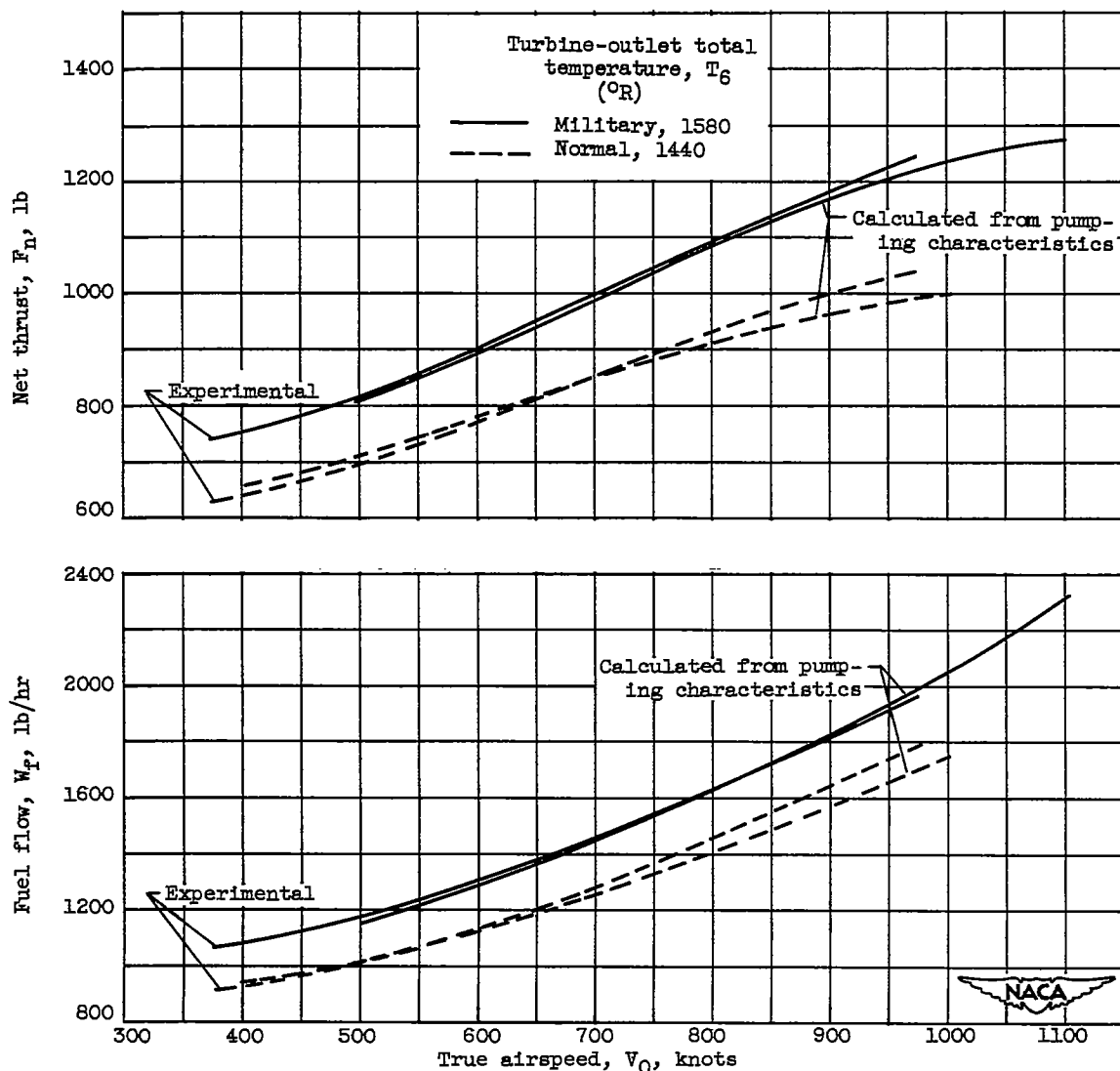


Figure 13. - Variation of net thrust and fuel flow with flight speed obtained from experimental data and data calculated from pumping characteristics. Altitude, 60,000 feet; engine speed, 7260 rpm.

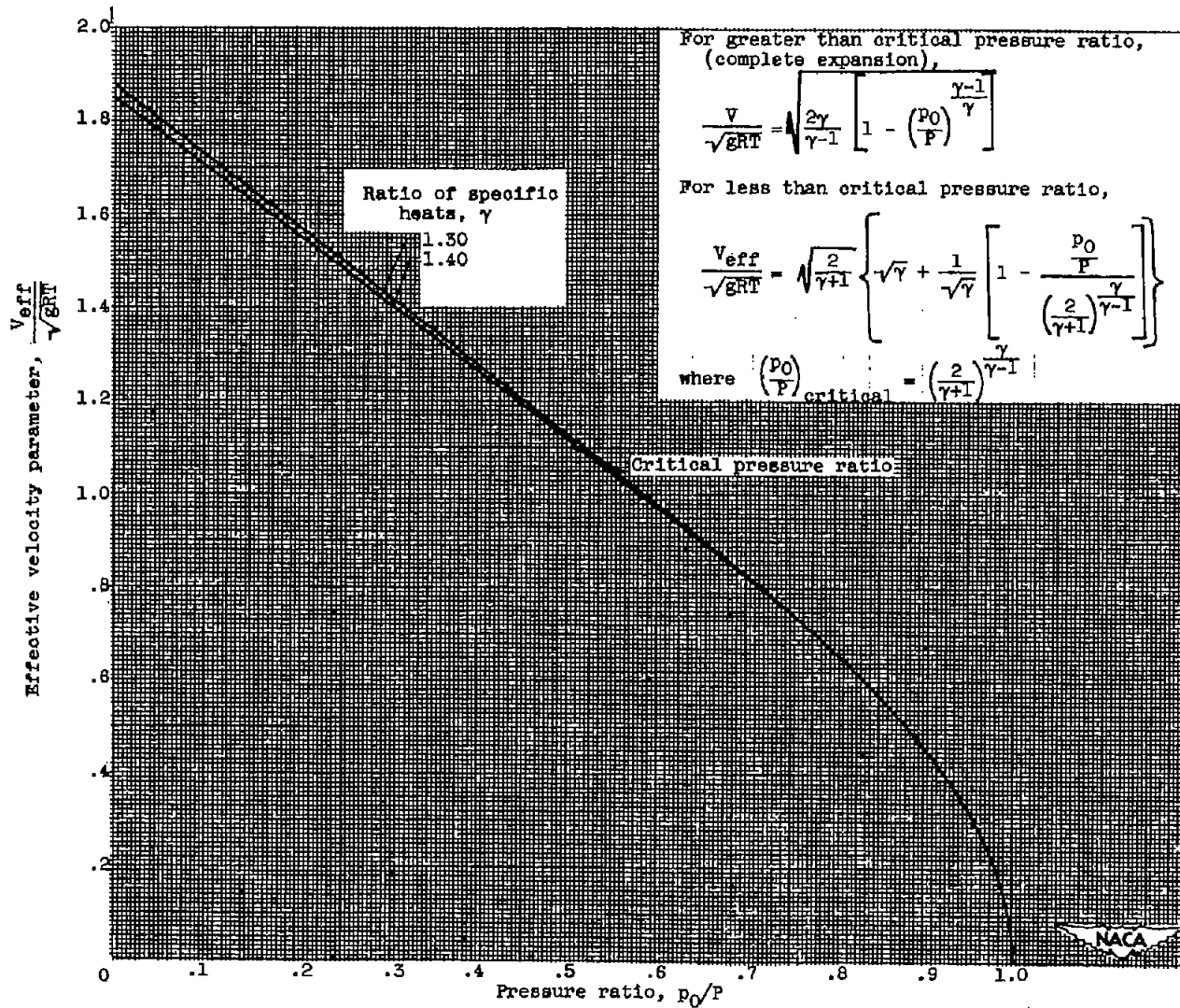


Figure 14. - Variation of effective velocity parameter with pressure ratio for convergent nozzle.

SECURITY INFORMATION

NASA Technical Library



3 1176 01435 6456